NASA-CR-159,519

C77-1148/501

NASA-CR-159519
19790019804

ANALYSIS AND PRELIMINARY DESIGN OF OPTICAL SENSORS FOR PROPULSION CONTROL

INTERIM REPORT

CONTRACT NAS3-21005

JANUARY 23, 1978

PREPARED FOR NASA-LEWIS RESEARCH CENTER, CLEVELAND, OH 44135

Authors: K. A. James
W. H. Quick

Rockwell International
Electronics Research Center
3370 Miraloma Avenue
Anaheim, California 92803

32 3 3 CN/NAS3-21005
DISPLAY 32/2/3
79N27975*# ISSUE 18 PAGE 2476 CATEGORY 74 RPT#: NASA-CR-159519
C79-386/501 CNT#: NAS3-21005 /9/01/23 90 PAGES UNCLASSIFIED
DOCUMENT
UTTL: Analysis and preliminary design of optical sensors for propulsion control --- temperature sensors TLSP: Final Report
AUTH: A/JAMES, K. A.; B/QUICK, W. H.; C/STRAHAN, V. H.
CORP: Rockwell International Corp., Anaheim, Calif. CSS: (Electronics Research Center.) AVAIL.NTIS SAP: HC A05/MF A01
MAJS: /*ENGINE CONTROL/*FIBER OPTICS/*REMOTE SENSORS/*TEMPERATURE SENSORS
MINS: / DIGITAL SYSTEMS/ FABRY-PEROT INTERFEROMETERS/ PHOSPHORESCENCE/ PULSE DURATION MODULATION/ SPECTRUM ANALYSIS/ TRANSDUCERS
ABA: A.R.H.
ABS: A fiber-optic sensor concept screening study was performed. Twenty sensor subsystems were identified and evaluated. Two concepts selected for further study were the Fabry-Perot fiber-optic temperature sensor and the pulse-width-modulated phosphorescent temperature sensor. Various designs suitable for a Fabry-Perot temperature sensor to be used as a remote fiber-optic transducer were investigated. As a result, a particular design was selected and constructed. Tests on this device show that spectral peaks are produced from visible white light, and the change in wavelength of the spectral peaks produced by a change in temperature is consistent with theory and is 36 nm/C for the first order peak. A literature search
ENTER:

ABSTRACT

This report considers twenty fiber-optic sensor subsystems. Depending on application requirements, various combinations of these subsystems can be used to form a sensor system with a digital transmission format which is unaffected by power interruptions, etc. The subsystems are divided into three groups--light source, sensor and detector.

All these subsystems, and the systems which are obtained by combining them, have certain desirable features and advantages. At least three of these systems are not only extremely promising, but are diverse enough in concept to make a further "narrowing down" to one "best" system for future study a very difficult task. The authors have converged on these three systems for further study because they embody the key principles involved in the concepts used for all of the twenty subsystems. These three systems are as follows:

A. Interference filter with temperature-dependent geometry utilizing color modulation.

B. Luminescent material with dependent emission decay time utilizing pulse-width modulation.

C. Point source of light with pressure-dependent motion utilizing a Holographic Processor to convert motion to color multiplex.

TABLE OF CONTENTS

ILLUSTRATIONS

TABLES

1. INTRODUCTION

1.1 PROBLEM

Present sensor technology has not kept pace with the data accumulation and reduction capability of modern microelectronics. Available sensors are bulky, costly and not readily compatible with digital microprocessing electronics. A means of monitoring aircraft engine status--e.g., temperature, pressure, flow rate, etc.--using sensors which are as reliable, rugged and inexpensive as semiconductor components will greatly enhance aircraft system performance. Such sensors, however, must withstand the hostile environments encountered by aircraft systems. Since most aircraft environments are subject to electromagnetic interference and hazardous gas atmospheres, an all-optical sensor concept for aircraft status monitoring is highly desirable.

1.2 OBJECTIVE

The objective of this contract is to identify innovative, promising concepts for passive, digital-compatible optical sensors, and to define the technology base required for their development. The intended application for these sensors is in digital electronic propulsion control systems for jet engines.

1.3 BACKGROUND TO SOLUTION

Recent advances in the field of micro-optic systems--i.e., fiber and integrated optics--have led to their introduction into military aircraft. Fibers are competing with electronic communications because of many advantages they possess over conventional data links. Such advantages include:

1. Immunity to electromagnetic interference.
2. Smaller, lighter and less expensive than electronic components.
3. Safe operation in a hazardous atmosphere.
4. Optical signals can be transmitted across bulkheads and gaps in the transmission path with no special considerations.

All these advantages apply when one considers utilizing fiber optics for aircraft engine propulsion sensors. The fundamental disadvantage arises when one realizes that sensing functions are inherently analog, while data transmission and processing are digital. Thus, the analog sensing function ideally will be converted to a digital signal at the sensor. The problem of analog signal variations due to fiber motion and random connector losses will then be avoided.

Fiber-optic sensor systems should have a digital transmission format and should be independent of intensity variation; therefore, a limit exists on the number of light wave transmission parameters which can be utilized. These constraints do not limit the number of parameters that can be used for sensing.

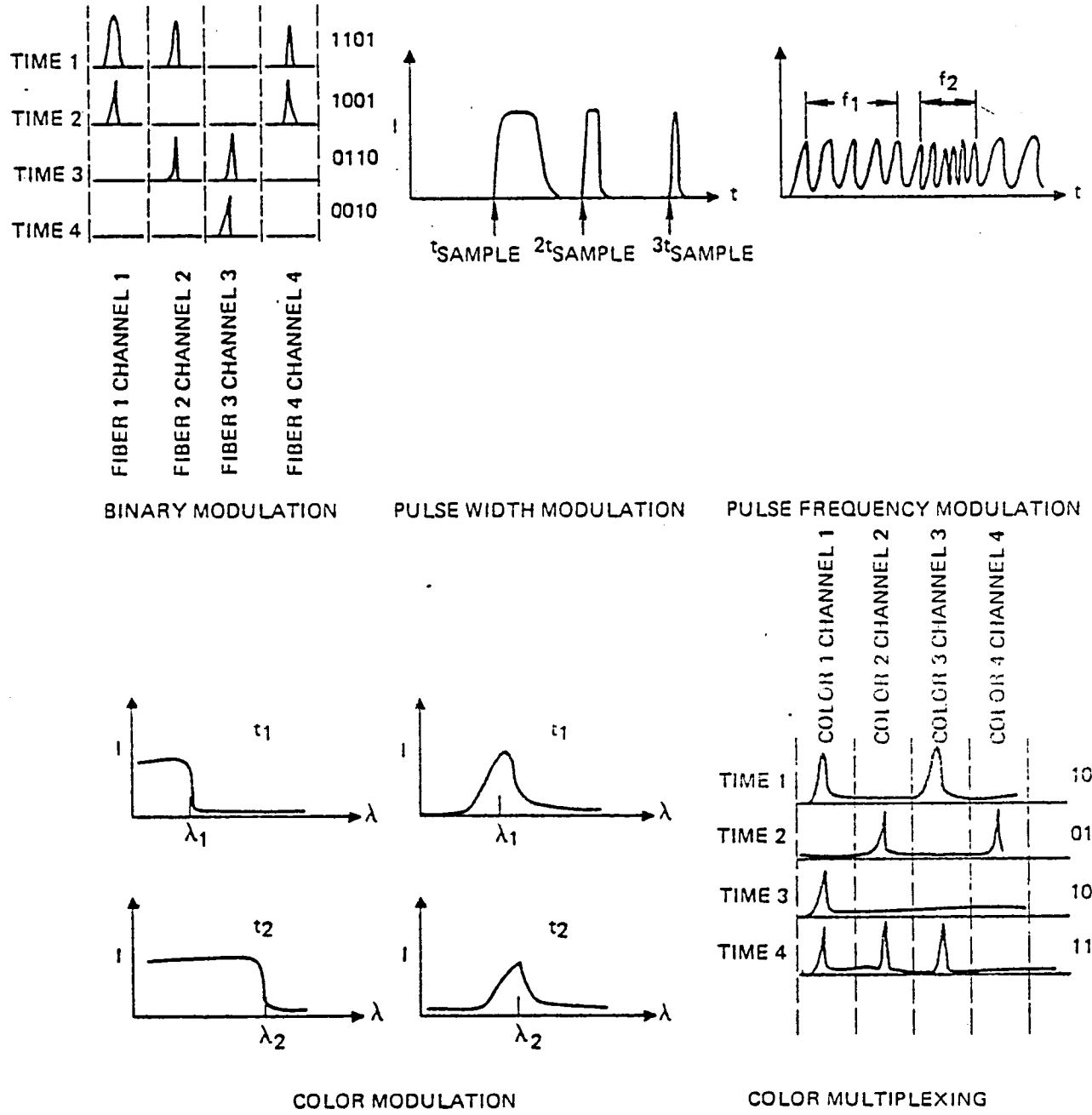

Figure 1.3-1. Fiber Sensor Modulation Formats

If single mode fibers were to be used, all five (5) characteristics of light could be applied to digital transmission; i.e., amplitude, intensity, wavelength, phase and polarization. However, the use of the more practical multimode (N > 1000) fiber restricts transmission schemes to digital intensity modulation (pulse width, pulse frequency, etc.), wavelength (or color) modulation and color multiplexing. These three basic format concepts are shown in Figure 1.3-1.

Even though some of the above-mentioned parameters, e.g., polarization, cannot be used for transmission, they can be used for sensing and then can be converted to a useful transmission parameter. For example, a material which alters polarization as a function of temperature can be sandwiched between crossed polarizers and, hence, can sinusoidally modulate intensity as a function of temperature. By using a number of these sensors--each with a different temperature resolution--a digitally encoded intensity signal can be generated and transmitted.

This example and the above discussion suggests a handy "black box" format for discussing fiber optic sensor systems (see Figure 1.3-2). The first box represents the light source or means by which the signal (to be modulated by environmental parameter and transmitted over the fiber) is generated. The second box represents the sensor subsystem and has two components--the environmental parameter to light wave parameter transducer and if needed, the light wave parameter to transmission parameter converter. The last box represents the subsystem which converts the digitized optical signal to a digital electrical signal.

This report is structured to correspond to the subsystem (boxes) shown in Figure 1.3-2. Tables 1.3-1, 1.3-2 and 1.3-3 indicate the light source, sensor and detector subsystems considered individually in the subsections of the technical discussion.

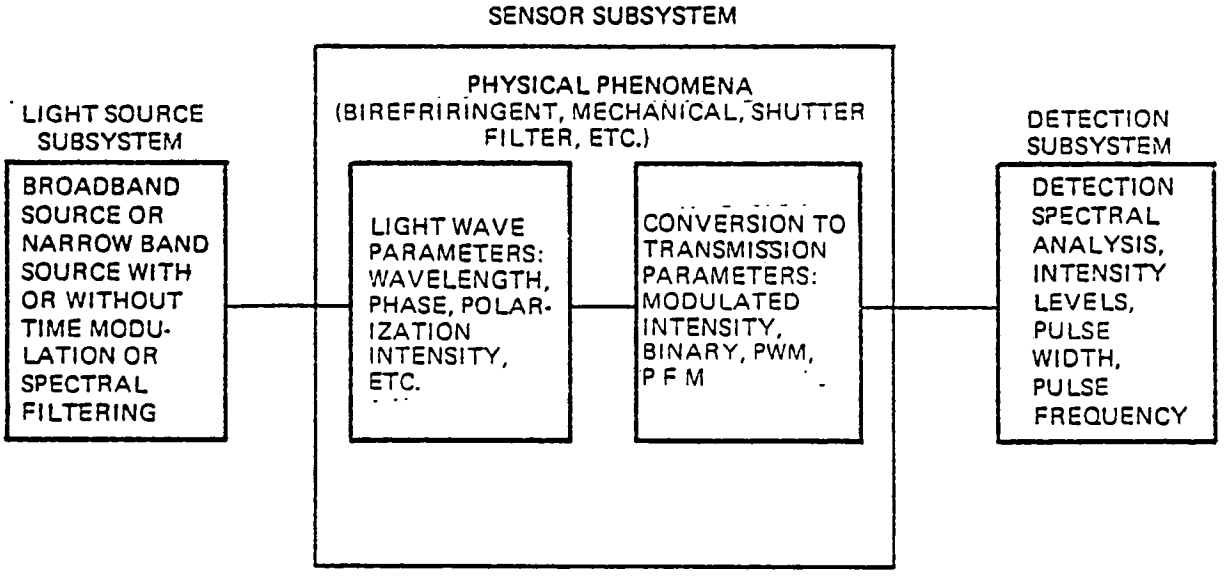

Figure 1.3-2. Fiber Optic Sensor Systems

LIGHT SOURCE	APPLICATION	SOURCE	SECTION
Narrowband	Binary, Pulsewidth, Pulse Frequency	Light-emitting diodes (direct bandgap) Laser Laser diode	2.1.1
Broadband	Spectral modulation eg, color modulation or or multiplexing	Incandescent Light-emitting diode (indirect bandgap)	2.1.2

Table 1.3-1 Light Source Subsystems

PHYSICAL PHENOMENA	OPTICAL PARAMETER EFFECTED	CONVERSION TO TRANSMISSION PARAMETERS	TRANSMISSION	SECTION
Temperature changes birefringent characteristic of crystal	Plane of polarization rotated	Using crossed polarizers at front and back of crystal causes sinusoidal variation in intensity. Using many sensors of different resolution yields digitally coded channels.	Color Multiplex or Coherent Bundle	2.2.1
Temperature or presssure causes luminescent decay of variable period	Intensity pulsewidth varies	None	Pulsewidth Modulation	2.2.2
Temperature or pressure causes material to luminesce at different wavelengths	Wavelength varies	None	Color Modulation	2.2.3
Pressure and/or temperature change filter character of semiconductor bandgap	Wavelength of high pass filter varies	None	Color Modulation	2.2.4
Pressure or temperature change dispersion crossings in anisotropic material causing coupling of polarization modes.	Wavelength of bandpass filter varies	None	Color Modulation	2.2.5
Multiple beam interference filter (multilayer and Fabry Perot) geometry with temperature pressure	Wavelength of bandpass filter varies	None	Color Modulation	2.2.6
Vibration or flow rate uses excitation of resonant frequency of particular length fiber.	Intensity pulse rate varies	None	Pulse Rate Modulation	2.2.7

Table 1.3-2 Sensor Subsystems

PHYSICAL PARAMETER	OPTICAL PARAMETER EFFECTED	CONVERSION TO TRANSMISSION PARAMETERS	TRANSMISSION	SECTION
Temperature or pressure -- uses Raman-Nath phase grating -- geometry variations	Wavelength spectral positional shift	None	Color Modulation	2.2.8
Temperature and pressure -- varies Bragg diffraction	Wavelength spectral positional shift	None	Color Modulation	2.2.9
Environment induced mechanical motion of optical shutter	Intensity switched on and off by shutter.	Shutter is binary (e.g., Gray scale) coded to produce digital word corresponding to environment.	Binary Modulation or Coherent Bundle	2.2.10
Environment induced mechanical motion of optical shutter	Intensity switched on and off by shutter.	Dispersion assigns color channel to each intensity modulated signal.	Color Multiplexed	2.2.11
Environmentally induced motion of point source of light	Position of light source	Holographic processor converts source position to color or binary signal	Color Multiplex or Coherent Bundle	2.2.12
Environmentally induced motion of point source	Position of light source	Variable bandgap semiconductor used to vary spectrum	Color Modulation	2.2.13

Table 1.3-2 Sensor Subsystems (Continued)

DETECTOR	QUANTITY DETECTED	METHOD	SECTION
Digital amplitude	Binary (including Gray code) bits on individual filters	One photocell for each bit	2.3.1
Pulsewidth	Time duration of pulse	Level ratio discrimination and gated counter	2.3.2
Pulse frequency	Frequency of light pulses	Signal from photocell analyzed electrically	2.3.3
Spectral analysis	Color modulated or multiplexed signal	Dispersing prism or grating, graded interference or conventional filter, etc., and CCD photocell array	2.3.4
Holographic processor	Binary or color modulated or multiplexed signal on incoherent bundle	Hologram translates position or color signal to pattern on photocell array	2.3.5

Table 1.3-3 Detector Subsystems

2.0 TECHNICAL DISCUSSION

This section is organized according to the black box representation of a sensor system in Figure 1.3-2. Three separate sensor subsystems--light source, sensor and detector--are each considered in a separate subsection. Such a format allows for condensing the vast number of sensor systems obtained from the various allowable subsystem combinations and permutations.

2.1 LIGHT SOURCE SUBSYSTEM

Since the light source subsystem is the starting point in analyzing a sensor system, it will be considered first. Typically, the light source subsystem will be the least complicated subsystem of the sensor structure.

2.1.1 Narrowband Light Source. This light source is usually required for intensity oriented transmission schemes (binary, PWM, PFM). Actual devices available for use include direct bandgap, binary or tertiary semiconductor light light emitting diodes (either "super-radiance" or laser). These sources might require modulation depending upon transmission scheme.

2.1.2 Broadband Light Source. This light source is usually required for spectral-oriented transmission schemes (color modulation, color multiplexing). Devices with such spectral output include light emitting diodes with indirect bandgaps or incandenscent sources.

2.2 SENSOR SUBSYSTEM

2.2.1 Temperature Sensor Utilizing Birefringent Crystals

The distinguishing basic feature of the crystalline state, as far as optical properties are concerned, is the fact that crystals are generally electrically anisotropic; i.e., the polarization produced in the crystal by a given electric field is not a simple scalar constant times the field, but varies in a manner that depends on the direction of the applied field relative to the crystal lattice. One consequence of this phenomenon is that the speed of propagation of a light wave in a crystal is a function of the direction of propagation and the polarization of the light.

Generally, for most crystals, there are two possible values of the phase velocity for a given direction of propagation. These two values are associated with mutually orthogonal polarization of the light wave. Hence, crystals are normally termed double refracting (birefringent). However, not all crystals are birefringent. Symmetrical cubic crystals, such as sodium chloride, never exhibit double refraction.

A handy model to illustrate the anisotropic polarization of a crystal is shown in Figure 2.2.1-1. A bound electron is depicted as being attached to a set of fictitious elastic springs. The springs have different stiffnesses for different directions of the electron's displacement from its equilibrium position within the crystal lattice. Consequently, the displacement of the electron under the action of an external field depends on the direction of the field as well as its magnitude (also true of the polarization). In addition, the spring stiffnesses may be sensitive to temperature, causing electron displacement to vary not only with field and polarization, but also with temperature.

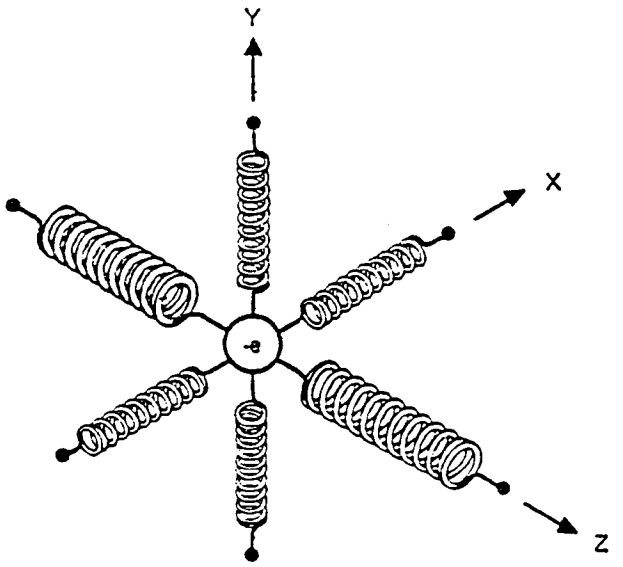

Figure 2.2.1-1. Model of Anisotropic Binding of Electron in Crystal.

Figure 2.2.1-2 is an application of this model to an intensity-modulated temperature sensor. A source with a broad spectrum is transmitted through a fiber and dispersed by a lens-prism system. The spectral components pass through the first polarizer. The resulting polarization vector is then rotated by the birefringent cell through an angle which is proportional to temperature. The second polarizing filter (the analyzer), causes the light intensity to vary sinusoidally with temperature. By using shorter birefringent cells, the other sensors are caused to have less sensitivity, so that each of the detected outputs represents a binary bit (e.g., "Gray code"). Then the color signals are mixed, transmitted by fibers back from the remote sensor and then separated and detected. This color-multiplexed sensor system is shown in Figure 2.2.1-3.

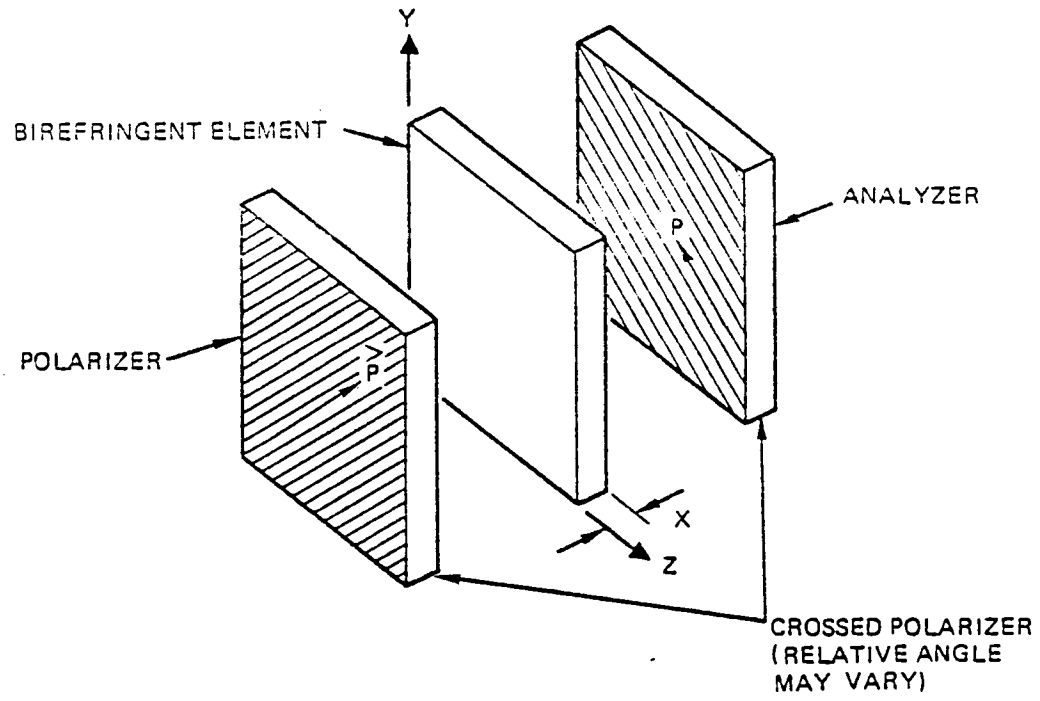

Figure 2.2.1-2. Birefringent Crystal Between Crossed Polarizers to Form Temperature Sensor Element.

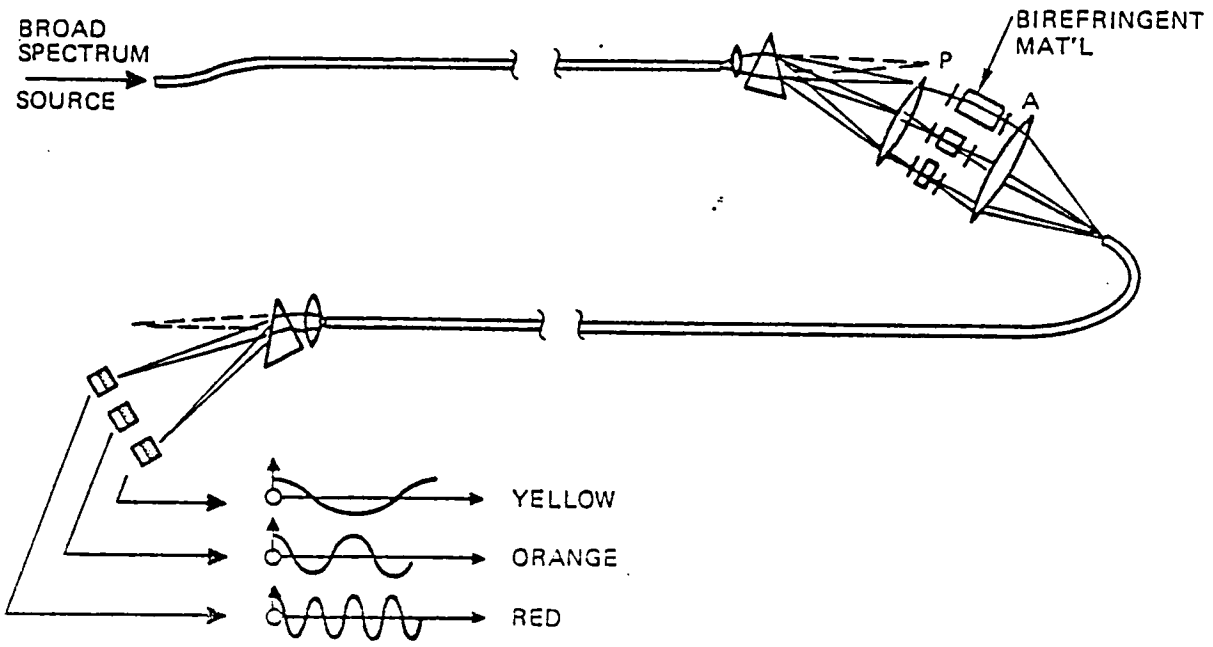

Figure 2.2.1-3. Birefringent Temperature Sensor Utilizing Color Multiplexing Transmission

2.2.2 Pulse-Width-Modulated Luminescent Temperature Detector

Of the many types of known luminescense,* the type which is of use here is photoluminescence, that is, luminescence which is excited by visible or near visible irradiation. Photoluminescence is divided into fluorescence and phosphorescence. Phosphorescence is the luminescence which occurs after the exciting radiation has been removed (in some definitions a length of time, such as 10 nanoseconds, after the exciting radiation has been removed is specified as the beginning of phosphorescence). Fluorescence is the radiation which occurs during excitation, and is normally of a different wavelength than the exciting radiation, but in the case of resonant fluorescence, may be of the same wavelength.

Because of possible difficulties of separating the exciting radiation from the luminescent radiation, it is the phosphorescent type of luminescence which is considered to be applicable to fiber-optic sensing.

Figure 2.2.2-1(a) shows the basic luminescent temperature sensor. It will be noted that physically this sensor is probably the simplest of the sensors being proposed. It consists of a pulsed light source, S, a phosphorescent tip, P, for sensing temperature at a remote location, and a photodetector, D, at the processing unit.

There are two basic physical characteristics of phosphorescent materials which are suitable for use as a temperature sensor. The shift in wavelength or color of the phosphorescent radiation will be discussed in the next section. The other effect, to be considered now, is the variation in the time constant of the decay of the phosphorescent radiation. This variation in decay time constant is illustrated in Figure 2.2.2-2.

Figure 2.2.2-2 shows the wide variation of time constant which can result from a change in temperature. It also gives some indication of other phosphor characteristics which will require study. This is a standard phosphorescent material, the structure being indicated on the drawing. This information is from reference (23). Note first the three solid lines which represent excitation by 4500 Å light. These decays are for the temperatures 169, 313, and 404°C. At 169°C, it is seen that the decay is to below 20% in a time period too short to measure on this graph, possibly one-tenth of a second or less. At a temperature of 313°C, it is seen that the output intensity falls by only 10% in one full second. The fact that this particular phosphor at this temperature has a long time constant should not be taken as an indication that quickness of response will be a problem; there are many thousands of phosphors available, and many of them have very rapid time constants. At the temperature of 404°C, it is interesting to note that the time constant has again shortened, so that there is a temperature of maximum time constant. This means that it will be necessary to select phosphors which are not double valued in terms of time constant in the temperature region of interest.

Two other factors which will require design considerations may be noted in Figure 2.2.2-2: First, it is noted that the time decay constant is a function of the wavelength of the exciting radiation. Second, it is noted that the

---

*Electro, thermo, auto, cathode, tribo, Roentgeno, iono, chemi, bio, cando, etc.

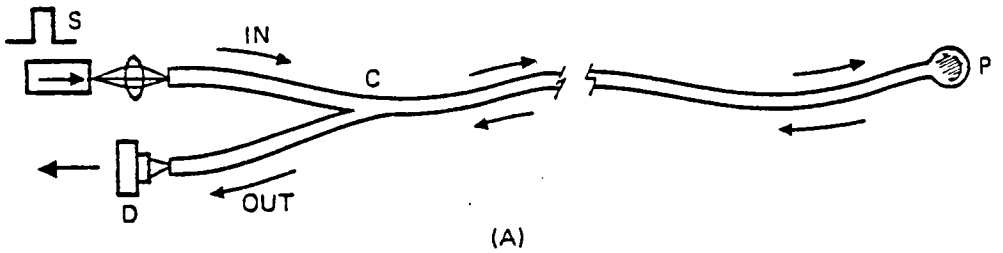

(A)

PULSED LIGHT SOURCE

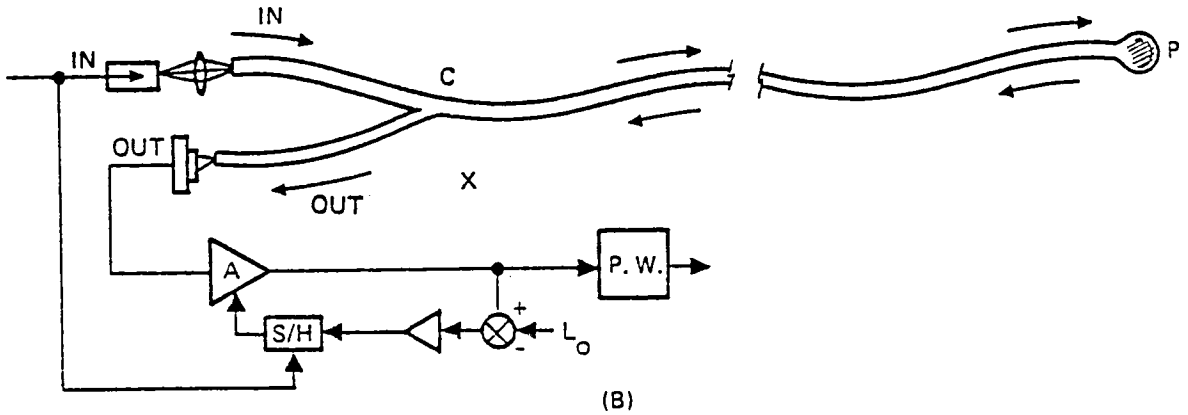

(B)

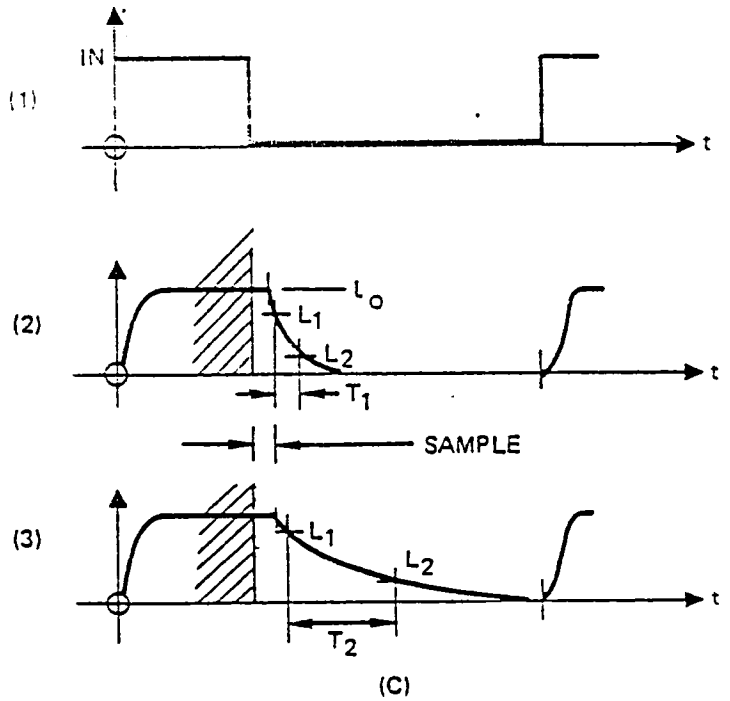

(C)

Figure 2.2.2-1. Pulse-Width-Modulated Luminescent Temperature Sensor.

initial phosphorescent output, L_o, compared to the value of L_o at 25°C, varies for the different conditions given on this plot. These values are given numerically after the temperature on the plot. A method of automatic gain control which is proposed to compensate for this variation in initial intensity, is described below in relation to Figure 2.2.2-1(b) and 2.2.2-1(c).

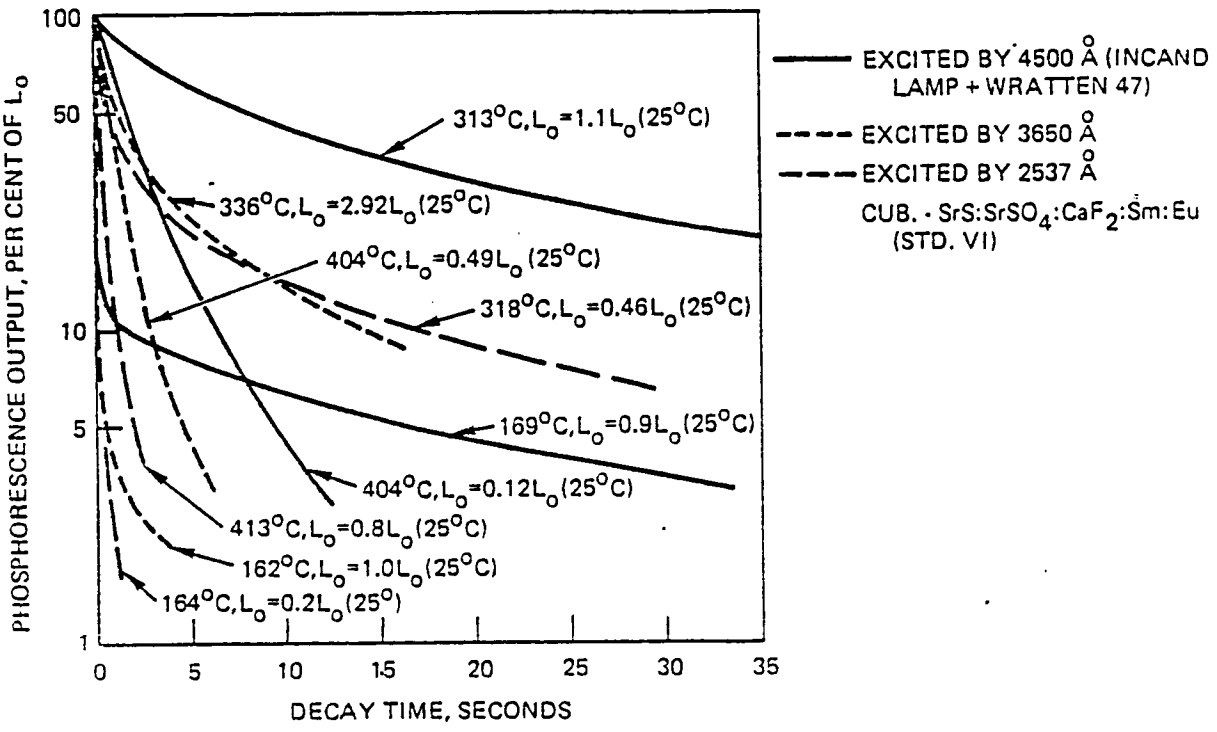

Figure 2.2.2-2. Phosphorescent Decay Characteristics of a Selected Luminescent Material

Coupler C can be made so as to couple most of the input light, labeled IN, to the transmitting fiber connecting to the phosphorescent tip. However, in all cases, some fraction of this light from the input will couple back into the output, labeled OUT, in Figure 2.2.2-1(b). Because the input light will be much more intense than the signal from the phosphorescent detector, even a small fraction of the excitation light being coupled back to the output could produce a signal larger than the signal which is to be sensed. Therefore, it is considered necessary to pulse the exciting source signal. In addition, if the decay transient is the quantity which is to be measured, the pulsing of the exciting source, S, is also necessary in order to create the transients which are to be measured. Figure 2.2.2-1(b) shows a block diagram of a scheme

which can be used to convert the pulse-width-modulated signal from the phosphorescent temperature detector to a usable output. Figure 2.2.2-2(c) shows waveforms which occur during this detection. Trace 1 shows the input pulsed light source. Traces 2 and 3 show output waveforms for two different temperatures of the phosphor.

The sequence of operation is as follows: During the input light pulse, the output of the phosphor builds up to a saturated value, as indicated in Trace 2 and 3. The area is partially shaded in the drawing because this actual value is not available for measurement due to the crosstalk in the bidirectional coupler, C. During the next period, labeled "sample" in Figure 2.2.2-1(c), the gain of the amplifier, A, is adjusted so as to bring its output to a value, L_o. This is accomplished by a block labeled S/H, for sample/hold, in Figure 2.2.2-1(b). The ending of the input pulse causes the sample/hold network to sample during the "sample" period following the input pulse. While this sampling is occurring, the output of the amplifier, A, is compared to the reference L_o. The difference between this output and L_o is passed through an amplifier and the sample/hold network to adjust the gain of the amplifier, A, in a negative feedback fashion, so as to null out this difference and cause the output of the amplifier, A, to adjust to the value of gain which brings its output to L_o. At the end of the sample period, the sample/hold device switches to the hold mode in which its output is a constant value, namely the value of the last sample. This maintains the gain of amplifier A at a constant value. Thus, referring to Figure 2.2.2-1(c) Trace 2, at the end of the sample period, will have the value L_o no matter what the actual output of the phosphorescent detector is, and no matter what the attenuation is through the line from the phosphorescent detector back through the coupler and into the photo output detector. As the light output of the photodetector decreases, the time which is required for this light output to pass from L_1 to L_2 is measured by the pulse width detector, which is simply a controlled counter. In Figure 2.2.2-1(c), Trace 2, this width is labeled T_1. In Trace 3, the temperature of the phosphor has changed and this decay period has changed to T_2. Because the amplitude is standardized at L_o, the pulse width could also be measured from amplitude L_o to amplitude L_2.

It is recognized that while this system is defined as a pulse width modulated system, the pulse observed (as seen in Figure 2.2.2-1(c), Trace 2 and Trace 3), does not have a sharp square pulse as is expected of a true pulse width modulated system. As has been pointed out, however, if the amplitude of the signal from the phosphorescent detector or the attenuation in the cable of that signal should change, the amplitude regulating system described in Figure 2.2.2-1(b) will compensate for the primary effects of such amplitude change.

2.2.3 Luminescent Temperature Sensor--Wavelength Detection

A second method of sensing the temperature of the phosphorescent tip is by the detection of the color temperature of the phosphorescent radiation. In this case, although pulsed excitation is not required for the purpose of initiating transients for pulse width modulation as before, pulsed excitation is nevertheless expected to be required in order to avoid the crosstalk of the excitation signal with the output. Alternatively, these two signals could be separated by establishing a wide frequency or wavelength separation between the exciting illumination and the phosphorescent illumination; in that case, the system would properly be called a flourescent detector rather than a phosphorescent detector.

In Figure 2.2.3-1, the light signal is shown originating at S, passing through the bidirectional coupler, C, passing to the phosphorescent (or fluorescent) temperature sensor, and returning to the detector, D, through the bidirectional coupler, C.

There are numerous ways of analyzing the wavelength pattern of the signal returning to the detector from the sensor. In this case, a hologram is shown. This hologram, as described elsewhere in this report, is designed to produce a binary signal, the value of the binary number being designed to indicate temperature to some suitable scale.

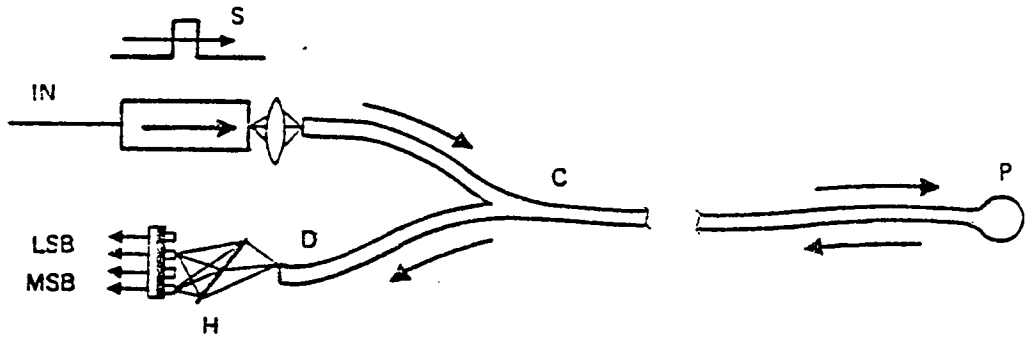

Figure 2.2.3-1. Wavelength-Modulated Luminescent Temperature Sensor.

2.2.4 Temperature and/or Pressure Dependent Semiconductor Filters

A prime sensor concept--color modulation--was introduced in the proposal. In this general concept a broad source spectrum is filtered by either a high- or low-pass filter, or, most ideal, a band-pass filter. Then, the detected spectrum is analyzed for cutoff or band-pass wavelengths. If these particular wavelengths of the filter elements are functions of environmental parameters, then the total system forms a fiber-optic sensor which is independent of intensity variations in the fiber.

A most straight forward manner of filtering involves semiconductor high-pass (relative to wavelength) filters. The presence of an energy gap in semiconductor materials makes them inherent optical filters. Photons of a given energy, and higher, can excite electrons from the valence band across the gap to the conduction band. These photons--of a given wavelength, λ_{co}, and shorter--are thus absorbed.

In the proposal for the contract, only crystalline semiconductor materials were considered. However, these crystalline structures are often difficult to deposit on various substrates. Further, some complicated compound semiconductors--although theoretically possible--have yet to be grown in sufficiently large crystals to allow for experimentation and evaluation. The fabrication advantages of amorphous semiconductor films over crystalline films include ease of fabrication and relaxed requirements on lattice constant matching with a variety of substrates. However, some differences in optical properties between the crystalline and amorphous states of a semiconductor do exist.

Many features of the crystalline semiconductor exist in the amorphous state. There is a filled valance band, roughly derived from bonding orbitals, and an empty conduction band derived from antibonding orbitals. In a pure, non-vibrating crystal, and in the one-electron approximation, the wave functions in the two bands may be written as the product of a plane wave of definite wave vector, $\vec{k}$, and a function having the periodicity of the lattice. In any real crystal, however, there will be defects (e.g., impurities, vacancies, intersitials, dislocations), which scatter the Bloch waves, so that the wave vector, $\vec{k}$, is only an approximate quantum number characterizing the states. In the amorphous material, $\vec{k}$ is not a good quantum number for the electronic states. Some remnants of $\vec{k}$-conservation may persist, however, in that states in a given energy range may contain wave vectors associated with particular with particular portions of the Brillouin zone of the ordered structure.

The rough features of the density of states will generally be the same in the amorphous material as in the crystalline, provided that the short-range ordering of the atoms is similar for the two cases. Sharp features of the crystalline density of states, arising from critical points in the Brillouin zone, where there is a vanishing of the gradient of the energy value with respect to wave vector, would, of course, be considerably smoothed out in the amorphous system. Corresponding to the energy gap in the crystal, there will be a quasi-gap in the energy band of amorphous material, where the density of states is much smaller than in the valence and conduction bands (see Figure 2.2.4-1).

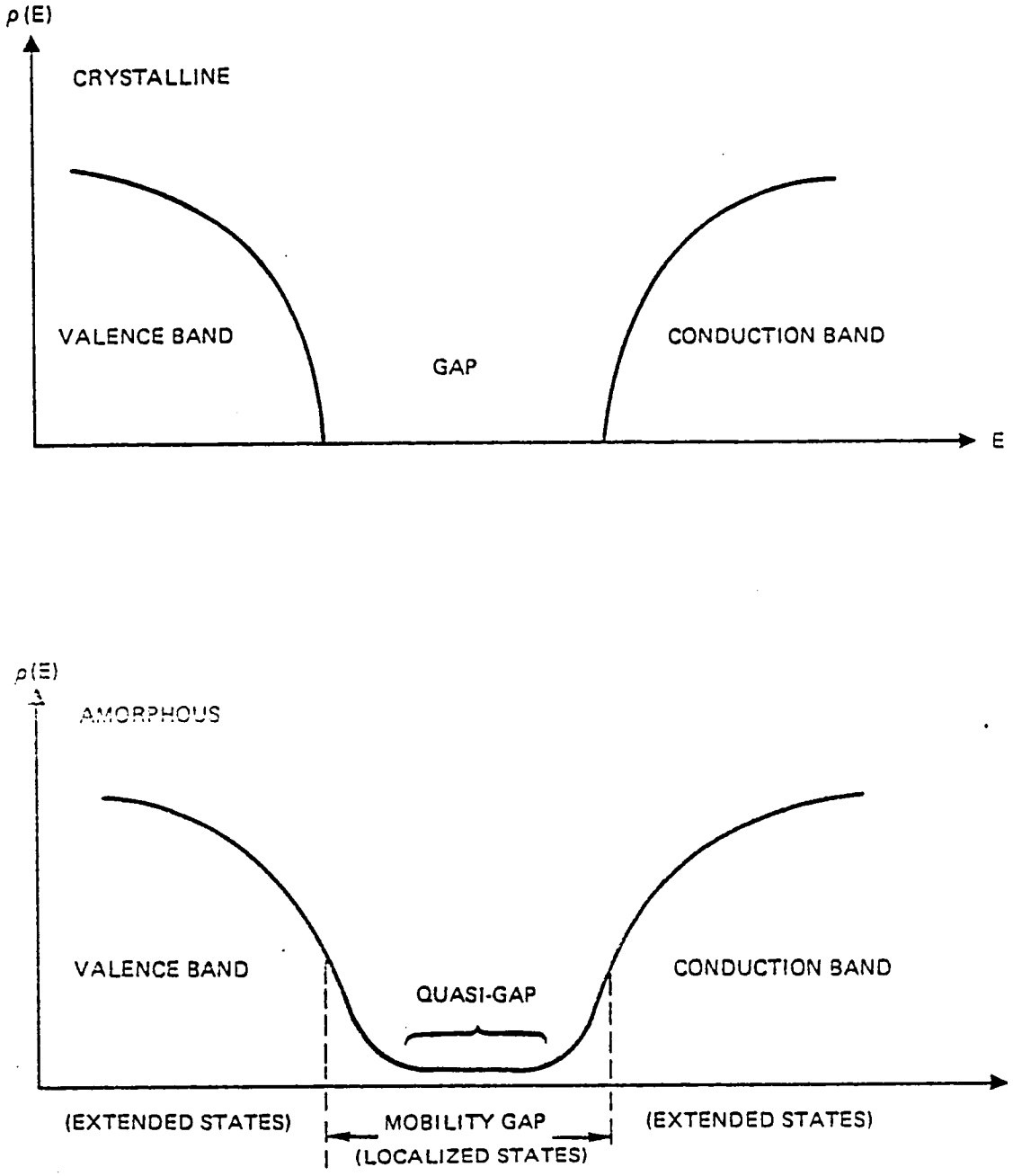

Figure 2.2.4-1. Schematic Density of States for a Crystalline and an Amorphous Semiconductor.

Principal Optical Absorption Band -- A typical example of the difference in optical properties between crystalline (c) and amorphous (a) solids is shown in Figure 2.2.4-2.

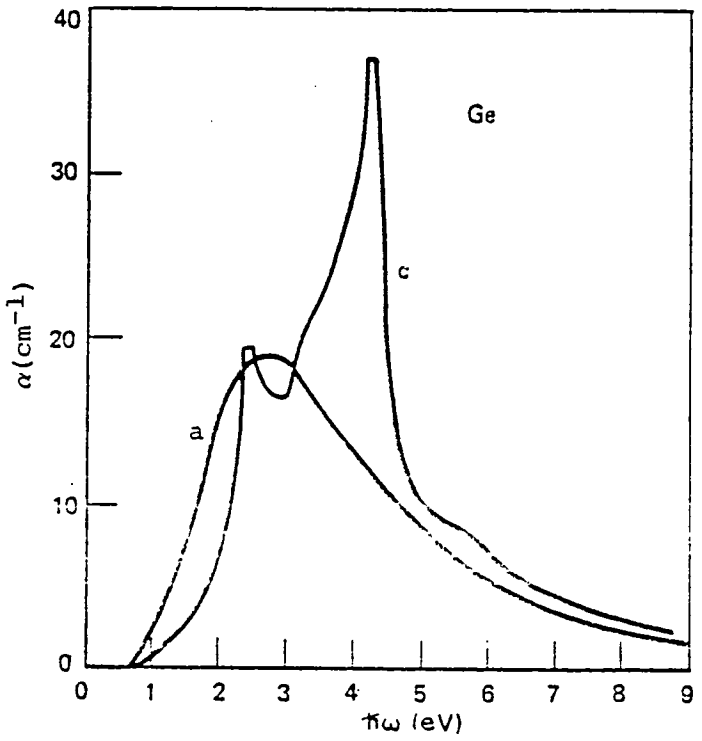

Figure 2.2.4-2. Principal optical absorption band of a a-Ge (curve a) and a c-Ge (curve c).

The principal absorption band of a-Ge is situated approximately in the same energy range as that of c-Ge, but it lacks the sharp structure characteristic of crystals. This is easily understood: with loss of the long range order, the $\vec{k}$ vector ceases to be a good quantum number and is only partially or not at all conserved during optical transitions.

Absorption Edge -- In contrast to the principal absorption band, the shape and energy of the absorption edge often depends on the preparation and thermal history of the samples (a structure-sensitive property), in particular,

in thin films. Figure 2.2.4-3 shows the dependence of the absorption constant of a-Ge in the region of the absorption edge on the temperature of annealing. The pressure shifts of the edge of amorphous Ge and Si are different from the shifts of any of the gaps in the crystal. Similarly, as in crystalline semiconductors, the definition of the absorption edge energy, E_g^{opt}, requires some knowledge or at least some theoretical assumptions, about the absorption processes in the region in question.

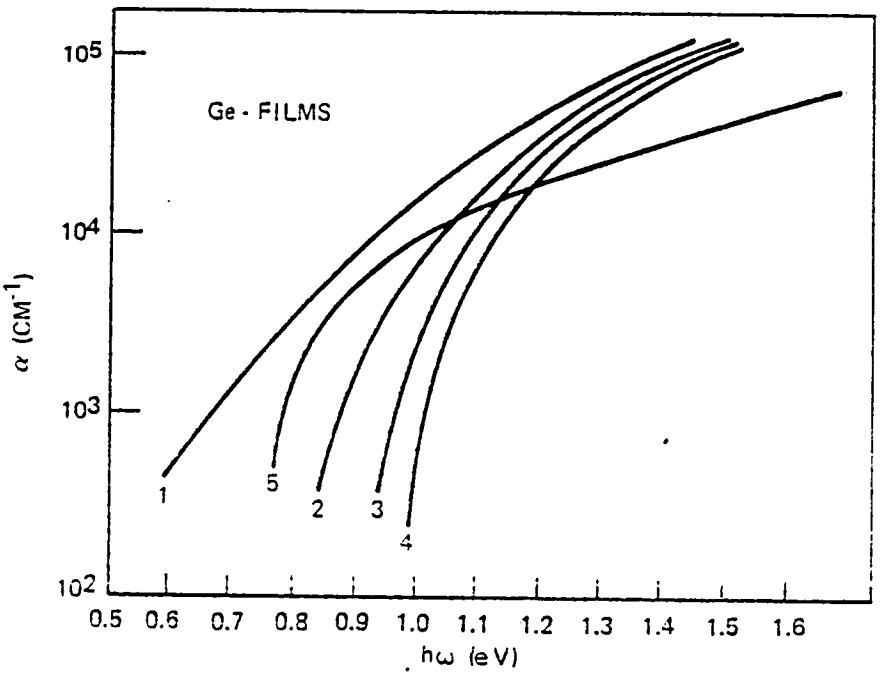

Figure 2.2.4-3. Dependence of the absorption edge of a-Ge on the temperature of annealing. Curve 1: deposited at 20°C, non-annealed. Curves 2, 3, 4 and 5: annealed at 200, 300, 400 and 500°C, respectively. During the annealing at 500°C, the sample crystallized.

An example of an amorphous semiconductor material which can be used as a temperature sensitive high pass filter for a fiber-optic, color-modulated sensor is shown in Figure 2.2.4-4. Amorphous Selenium will absorb variable wavelength radiation over a range from -200°C to 400°C.

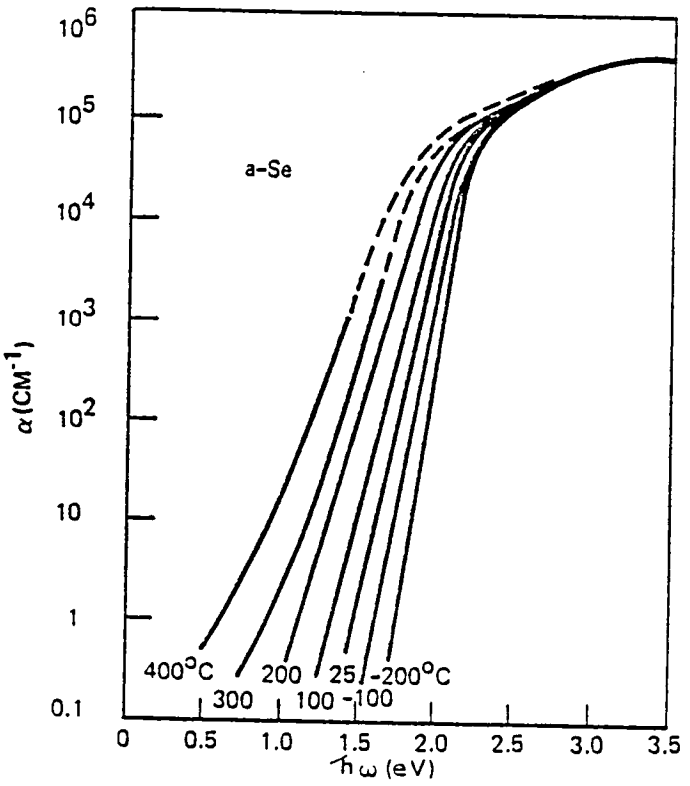

Figure 2.2.4-4. Absorption Edge of a-Se at Various Temperatures

One final point to be made about amorphous semiconductor technology is that it has potential application in forming teritiary and quarternary semiconductors. These materials have much greater versatility as environmental parameter to optical filter transducers than single element semiconductors.

2.2.5 Narrow-Bandpass Filters Utilizing Coupled Polarized Modes

For optimum discrimination at the spectral detector of a color modulated sensor system, a bandpass filter sensor element--rather than a low- or band-pass filter sensor element--should be used. Most contemporary optical band-pass filters, however, are high-cost microfabricated elements of very precise dimensions (e.g., multilayer interference filters or Fabry-Perot cavities). Recently, however, a narrow band filter which consists of a single crystalline material has been developed. This device has the potential for being formed more easily and fabricated more economically, while being more sensitive to environmental parameters than the previously mentioned types of band-pass filter sensor elements.

One promising sensor concept involves the coupling of polarized light waves in mixed crystals. In hexagonal semiconductors, e.g., ZnO and CdS, at energies below band gap, light polarized perpendicular to the optical axis is strongly absorbed while light polarized parallel to the axis is readily transmitted, as shown in Figure 2.2.5-1. This absorption cannot be due to transitions between two discrete electronic energy levels, but results from a coupling of energy from the transmitted mode (parallel to optical axis) to the absorbing mode (perpendicular to the axis). This coupling would ordinarily not take place; however, ZnO and CdS have several crossings of the index of refraction curves--n_y and n_z. At these crossings, the anisotropic crystal becomes optically isotropic and the two types of polarized modes have the same phase velocities ("k" vectors), and thus are easily coupled. Since this coupling only takes place at energies (optical wavelengths) where the refractive index curves cross, it gives rise to discrete spectral absorption lines.

The problem of coupling two electromagnetic waves as discussed here is identical to the problem in mechanics of the coupling of two pendula by a weak spring, as shown in Figure 2.2.5-2. Suppose pendulum 1 is initially at rest, while pendulum 2 initially has some energy. Assume a negligible energy is stored in the spring and that damping is small. If $\omega_1 = \omega_2$, the energy will pass from pendulum 2 to pendulum 1 until finally pendulum 2 is at rest and all the energy that has not been dissipated will belong to pendulum 1. The energy will then flow slowly back to pendulum 2, etc. If $\omega_1 \neq \omega_2$ and if $\omega_1 - \omega_2$ is large compared to the frequency at which the energy is transferred between identical pendula, then long before pendulum 2 has transferred all of its energy to pendulum 1, the relative phase of the two pendula will change and the energy will begin to flow back to pendulum 2. Thus, the frequency of energy transfer will increase and the energy transfer will be far from complete. The equation describing the transferred energy is a function of time t for the two pendula with frequencies ω_1 and ω_2. The equation is the same for the transferred energy (but as a function of distance, x) through the crystal between two electromagnetic waves with wave vectors k_y and k_z. In the former case, the transferred energy is a function of $(\omega_1 - \omega_2)\, t$ while, in the latter case, it is a function of $(k_y - k_z) \cdot x$.

This phenomenon could be implemented in a band-pass filter used with crossed polarizers, or in a band-reject filter used with parallel polarizers. The filter wavelength may be altered by varying the temperature or by applying an external strain.

However, for ZnO or CdS, this variation occurs over a somewhat limited spectral range. Use of II-VI semiconductor materials can extend the spectral range to include the entire visible and near IR spectra. Such materials as $Cd_{1-x}Zn_x$ and $CdSe_{1-x}Te_x$ have graded band-gaps and, hence, a coupled light-wave filter can theoretically be operated in a spectral range of .4 μm to .9 μm. The temperature and pressure dependence of the band-gap of these materials have been investigated for applicability in color modulation sensor systems.

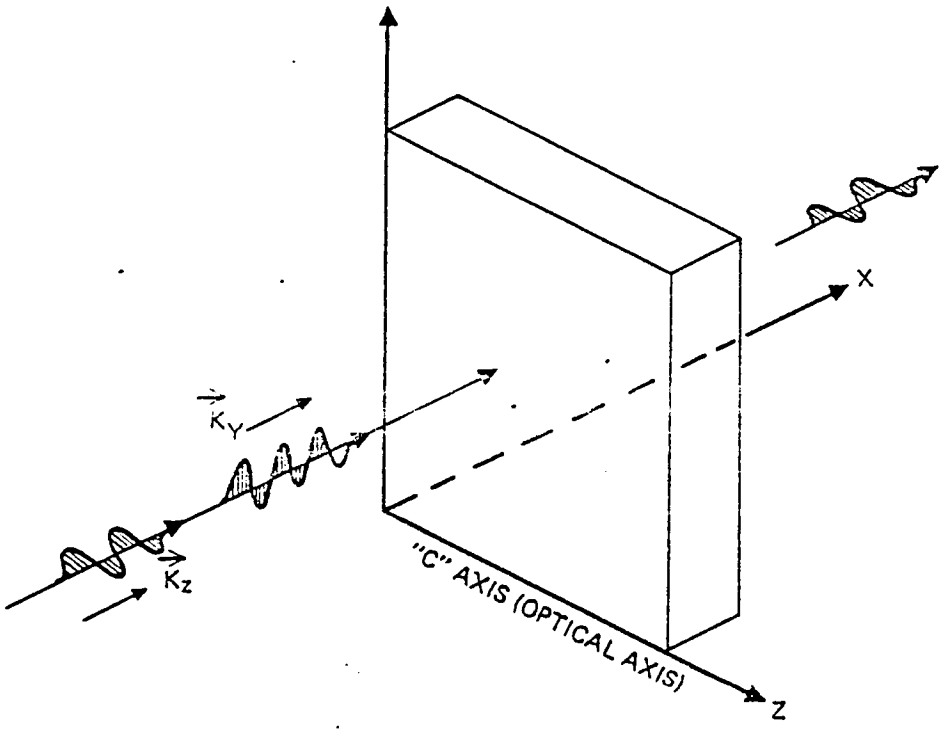

Figure 2.2.5-1. Propagation of Polarization Through Anisotropic Crystal

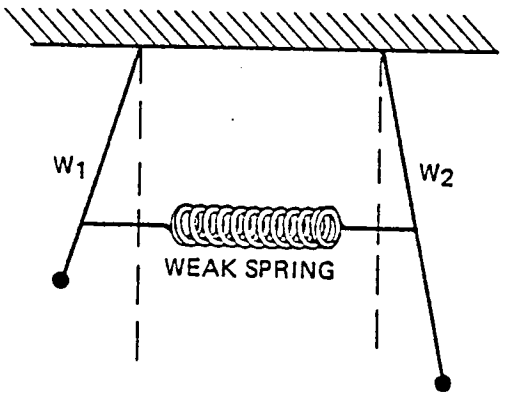

Figure 2.2.5-2. Coupled Pendulum Analogy to Coupled Polarized Modes

2.2.6 Multi-Beam Interference Sensors

Sensors may involve a multiplicity of reflections and splitting of a beam of light in a manner such that interference and support of the various components of a single light ray can occur a multiplicity of times. Such sensors have the desirable characteristic that the change in output can be a very sharp function of the wavelength. For example, in Figure 2.2.6-1, an entering beam of light is shown being partially transmitted and partially reflected a multiplicity of times. Because of a phase reversal which occurs when light is reflected from a more dense to a less dense medium (but does not occur from a less dense to a more dense medium), it is possible for the main reflecting beam, shown by dashed lines in Figure 2.2.6-1 to cancel at a gap which is equal to a multiple of half wavelengths. At the same time, the transmitted rays undergo an even number of reflections; so that even if there is a phase reversal, the even number of phase reversals produces no net reversal, and the transmitted components of light , at a half-wavelength gap, are in supportive phase and transmission occurs. When the reflectivity of the surface is relatively high, a very large number of reflections is required before the transmitted beam adds up to an amplitude close to the amplitude of the incident beam. Under this situation, even a very small difference in light frequency causes the transmission to drop drastically. The result is a device with a very narrow transmission band, in terms of light wavelength. Such a device is known as a Fabry-Perot etalon when the space between the two plates is held fixed, and a Fabry-Perot interferometer when the space between the plates can be mechanically varied.

In Figure 2.2.6-2, a type of construction which is visualized for this program, is shown. The steps of the construction are represented from Figure 2.2.6-2(a) through Figure 2.2.6-2(e). In Figure 2.2.6-2(a), the ends of two fibers are shown having been spherically terminated. In Figure 2.2.6-2(b), these two ends have been polished so that they form enlarged flat surfaces, perpendicular to the axis of the fibers, at the end of each fiber. In Figure 2.2.6-2(c), a step has been added to the fiber on the left. It is anticipatged that this step might be constructed by the cementing on of a small, solid cylindrical piece of glass or quartz. Alternatively , the raised step in Figure 2.2.6-2(c) may be formed by direct grinding procedures on this end. In Figure 2.2.6-2(d), a metal or other suitable washer-shaped spacer is shown applied around the step which was formed in Figure 2.2.6-2(c). In Figure 2.2.6-2(e), a variation in height has been produced so that the glass center is somewhat shorter than the metal spacer. It is very important that the plane surfaces of the spacer and the step in the fiber extension be very flat and parallel. A method which is visualized for accomplishing this is as follows. First the fiber end with the spacer attached, as in Figure 2.2.6-2(d) is polished off to a single plane across the spacer surface and glass or silica surface. It is important that this plane be extremely flat; the large number of reflections which occur in the Fabry-Perot interferometer or etalon increase the need for precision. (A flatness of 1/20 to 1/100 wavelength has been recommended for some Fabry-Perot applications. While the small size of the unit being discussed here makes handling, etc., more difficult, it also means that random flatness variations will be measured over a much smaller surface where there is less room for degrading variations. For example, if a large ordinary plate flat to 1/4 wave were to be examined on portions of its surface measuring only several hundred micrometers, the flatness on those individual surfaces would certainly be found to be much better than that measured over the entire surface).

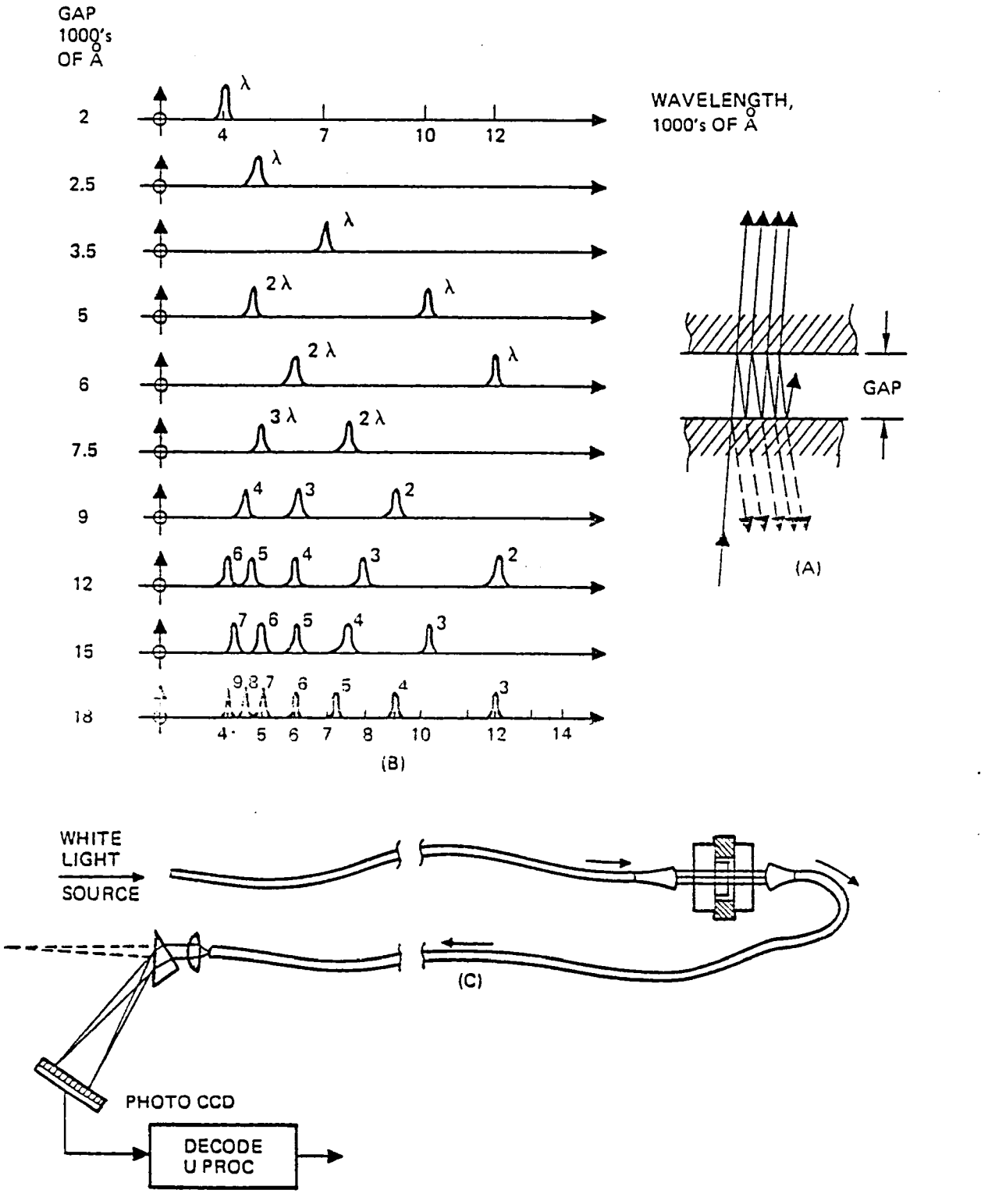

Figure 2.2.6-1 Application of Multiple-Beam Fringe Sensor

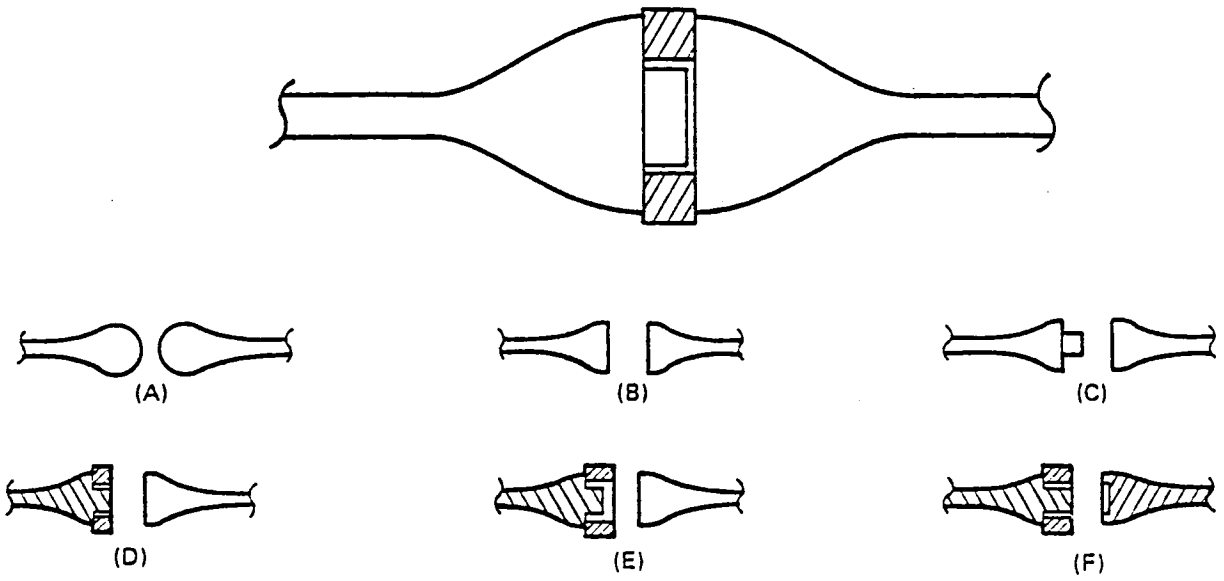

Figure 2.2.6-2. Multiple-Beam Fringe Sensor with Holographic Processor Detector

After the surfaces of the metallic spacer and fiber extension, Figure 2.2.6-2(d), have been ground to being flat and coincident, the difference in height, as shown in Figure 2.2.6-2(e), must be produced. One of the simplest ways of producing this would be to do the final polishing at a low temperature, lower than any temperature that is expected to be used by the instrument. The difference in expansion coefficients then will produce this height difference, when the components are brought to the operating temperature. Another method of producing this height difference would be the vapor deposition of a spacing material on the outer periphery. This spacing material,or the step produced in some other fashion, could be formed instead, on the matching hemisphere, as shown in Figure 2.2.6-2(f).

The devices just described may be visualized as a temperature sensor, wherein the spacer made of metal or other suitable material has an expansion coefficient larger than that of a glass or a quartz optical material. The same scheme may also be a pressure sensor, wherein the spacer is made of an elastic material suitable to the pressure range to be measured. In this case, the structure must be capable of maintaining the optical surfaces to a high degree of parallelism, a problem not expected to be difficult in the case of temperature sensing. A third application of this basic structure is the sensing of gas density by the measurement of its change in index of refraction. Gas,admitted to the gap between the surfaces, will cause the optical path length to change with the density and index of refraction of the gas. In this application, no metal or compliant space would be used.

An interesting means of sensing the change in optical characteristics of this device is by illuminating it with a white light source. In this case, only the wavelength or colors, for which the gap is equal to a multiple of half wavelengths, are transmitted. The transmitted spectra at different gaps are plotted in Figure 2.2.6-1(b). It is seen that the wavelength of the transmitted light increases as the gap increases. As the wavelength of the transmitted light moves out of the visible region and into the infrared, a new line appears in the visible region and moves toward longer wavelengths. This pattern is repeated as the gap continues to increase. Although at the larger gaps, the lines moving across the spectrum are a repetition of lines which moved across the spectrum at lower gaps, the entire spectrum is not duplicated. This is because additional lines appear during the repetitions. For example, at a gap of 6000 Å, the 2λ line appears at 6000. At 9000 Å the 3λ line also appears at 6000 Å, but in addition, 4λ and 2λ lines appear at 4500 Å and 9000 Å, thus uniquely distinguishing 9000 Å gap from the 6000 Å gap. At 12,000 Å, the 4λ line again appears at 6000 Å, but the rest of the pattern, again, is different from that at 9000 and 6000 Å.

Thus, with adequate decoding, it will be possible to detect the value of the gap over a range of many wavelengths. One possible means of decoding this information is by breaking the spectrum up with a dispersing prism, as is shown in Figure 2.2.6-1(c), detecting this spectrum by a photocell array, and examining this array in a microprocessor which stores the algorithm required for decoding this information. Alternatively, the decoding process could be part of the function of a larger microprocessor or computer.

The discussion elsewhere in this report, of the use of a Holographic Processor for the decoding of complex signals, suggests that this might be applicable to the present signal. Although there may be reasons why the signal may not be easily converted to any binary or Gray code binary signal, it seems apparent that the signal can be decoded into a binary electrical output of some suitably defined code. A difference in the application of the Holographic Processor here to the applications which are discussed in the section on the Holographic Processor is that information here is contained in wavelength or color, not in location of the beam as was the case in the other discussion. However, as discussed in the section on color multiplexing in relation to Figure 2.2.12-2, the hologram quickly becomes defocused when the color shifts, because at different wavelengths, the pattern of reinforcement changes. In addition, the sensitivity to color may be increased by using a thick-film hologram, of the type known as a Lippman-Bragg hologram. The thick-film hologram, operation at colors other than that for which particular image is designed, is interfered with by deviation of the wavelength from the spacing of portions of the hologram spaced through the thickness, that is, along the axis of the hologram.

It will be noticed that the Holographic Processor of Figure 2.2.6-3 differs from some of the others discussed, in that is it not a portion of the sensor but becomes a portion of the central processing unit.

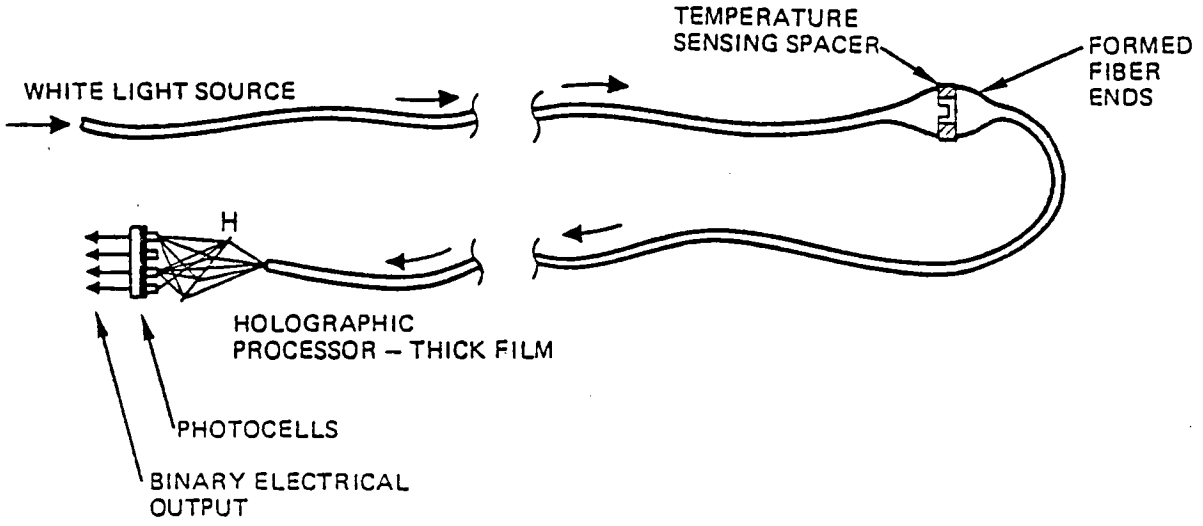

Figure 2.2.6-3. Steps in the Construction of a Multiple-Beam Fringe Temperature Sensor.

2.2.7 Vibration Sensor Using Pulse Frequency Modulation

Consider a fiber-optic vibration sensor where some form of vibration causes the fiber to oscillate and causes the fiber to be switched on and off. The fiber optic transmission system is not a digital "word" indicative of a position, but rather a pulse sequence whose frequency is indicative of physical vibration. One type of sensor which incorporates this frequency modulation concept is shown in Figure 2.2.7-1.

By using several fibers of the same cross-section but varying lengths, a wide range of vibrations can be monitored. The individual fiber sensors--constrained to oscillate in only one direction--are offset slightly from a light source fiber so that the light signal is normally off but oscillates when the fiber is resonating. The resonant frequency and bandwidth of the fiber is determined by its length, diameter and elasticity and the medium damping.

At the detection subsystem, the actual fiber from which the oscillating light signal emanates is irrelavent: only the signal frequency is important. Thus, incoherent fiber bundles can be used.

Some practical problems do exist with such a vibration sensor. One such problem is the possibility of fiber fatigue and loss of optical properties after long continued flexing. Little data is available on fiber bending at high mechanical frequencies for long period of time.

Another application of the oscillating fiber sensor with pulse frequency modulation is as a flow rate sensor. Hydrodynamics shows that a thin flexible cylindrical rod--similar to a fiber--will oscillate in a flow when a particular flow rate is present. Such oscillation is due to Von Karman vortex shedding. Initial analysis of this effect indicates that the vortex fabrication is suitable for flow velocity measurement over an intermediate range of Reynolds numbers relative to fiber diameter, above laminar flow, but below highly turbulent flow where the regular vortex pattern is lost.

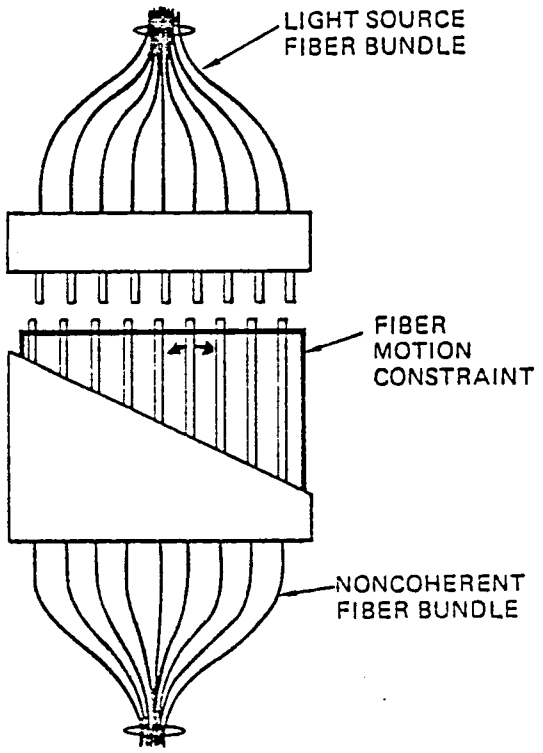

Figure 2.2.7-1. Fiber Optic Vibration Sensor

2.2.8 Raman-Nath Phase Grating Geometry-Variation Sensors

Various multilayer structures of alternating index-of-refraction layers can diffract light in two ways. One is the Raman-Nath type of light diffraction, which is essentially a phase grating phenomenon. The other is Bragg diffraction, which, although a special case of Raman-Nath, is more of a volume effect, in correspondence with Bragg diffraction of x-ray by a crystal lattice.

In a Raman-Nath phase grating, the output wavefront is phase modulated by the periodic change in the index of refraction. The resultant corrugated wavefront, in turn, causes many interference peaks in the far-field region with the angle of the m^{th} order given by

$$\sin\theta_m = m \frac{\lambda}{\Lambda} \qquad m = 0, \pm 1, \pm 2 \qquad (2.2.8\text{-}1)$$

where λ and Λ are the optical and mechanical wavelengths, respectively. The intensity of the m^{th} order interference peak is given as

$$\frac{I_m}{I_0} = J_m^2 (\upsilon) \qquad (2.2.8\text{-}2)$$

$$\upsilon = 2\pi\Delta n W/\lambda n_1 \qquad (2.2.8\text{-}3)$$

where W is the grating width and Δn the index difference between the grating layers. Note that in Equation 2.2.8-2, the intensity is independent of variation in Λ (Eq. 2.2.8-3).

A sensor formed by a Raman-Nath type grating must utilize the far field color pattern (Eq. 2.2.8-1) and an "Optical Lever" type of positional amplification, which shifts the spectrum. Thus, by monitoring the spectral component at one or two far field positions, color modulation can determine the variation in Λ due to environmental parameters. This simple sensor system, although adequate, can be vastly improved by monitoring all positions in the far field. The technique requires a form of Holographic Processing as described in Section 2.2.12.

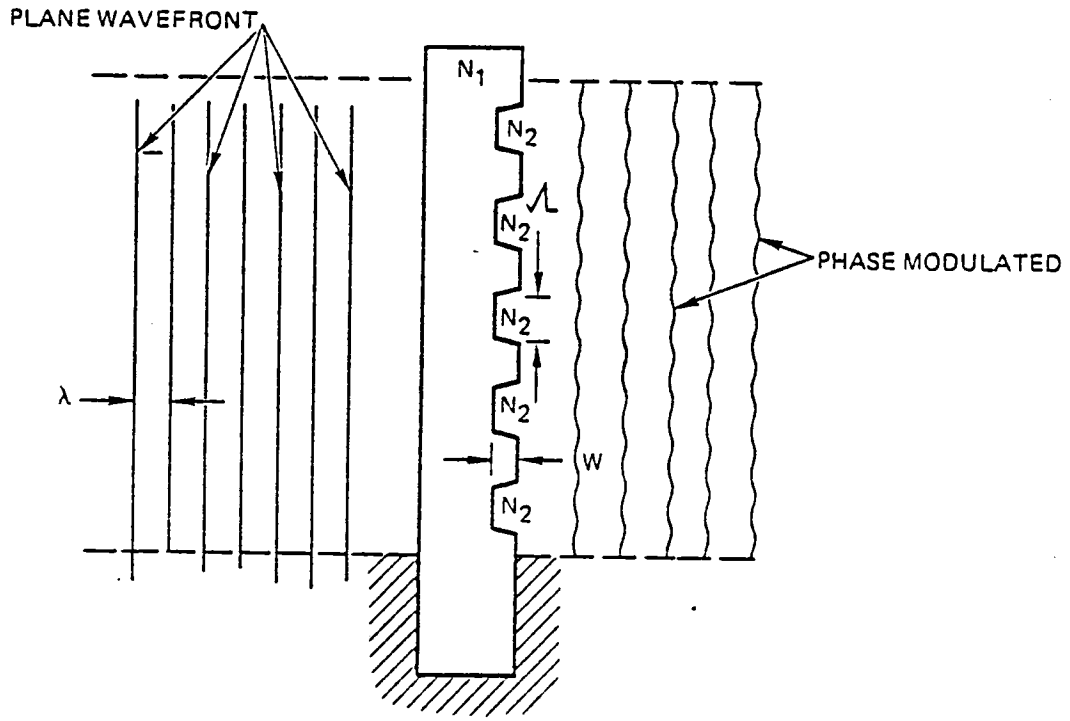

Figure 2.2.8-1. Raman-Nath Phase Grating Designed for Sensing Geometry Variation

2.2.9 Bragg Diffraction Sensor of Index of Refraction Change

As the width, W, of a grating increases or the mechanical wavelength, Λ, decreases, the diffracted light begins to be dominated by an amplitude modulation. This modulation arises from interferences in the light reflected due to the discontinuities in the refractive index, which can vary as a function of temperature or pressure.

The condition for the Bragg diffraction is given by

$$Q = \frac{2\pi\lambda W}{\Lambda^2} > 1 \qquad (2.2.9\text{-}1)$$

where λ and Λ are the optical and mechanical wavelengths, respectively, and W is the grating width. Note that λ is not the free-space wavelength but rather the optical wavelength in the medium with variable index n_1 (see Figure 2.2.9-1). This equation for Q can be considered as the number of individual grating elements in the grating having a width W transversed by the incident beam with an incident angle Θ where

$$\sin\Theta = \frac{\lambda}{2\Lambda} \qquad (2.2.9\text{-}2)$$

For Bragg diffraction, the value of Q must be larger than unity, so that the reflection from each grating element can be added constructively for the output of Bragg diffraction. The Raman-Nath region, where only the phase modulation of the incident beam is important, corresponds to $Q < 1$.

For stability of the structure in Figure 2.2.9-1, W must necessarily be much greater than Λ. Thus, the Bragg deflector requirement of 2.2.9-1 holds, and equation 2.2.9-2 specifies the angular distribution of the spectrum. The variation of n_1, due to an environmental parameter, will cause λ (and hence Θ) to vary with that parameter.

Sensor system concepts listed for a Raman-Nath phase grating (Section 2.2.8) apply to the Bragg Deflection--i.e., color modulation and Holographic Processing. The primary difference between the two phenomena is that the Raman-Nath structure is sensitive to geometry variations while the Bragg structure is sensitive to index of refraction variations.

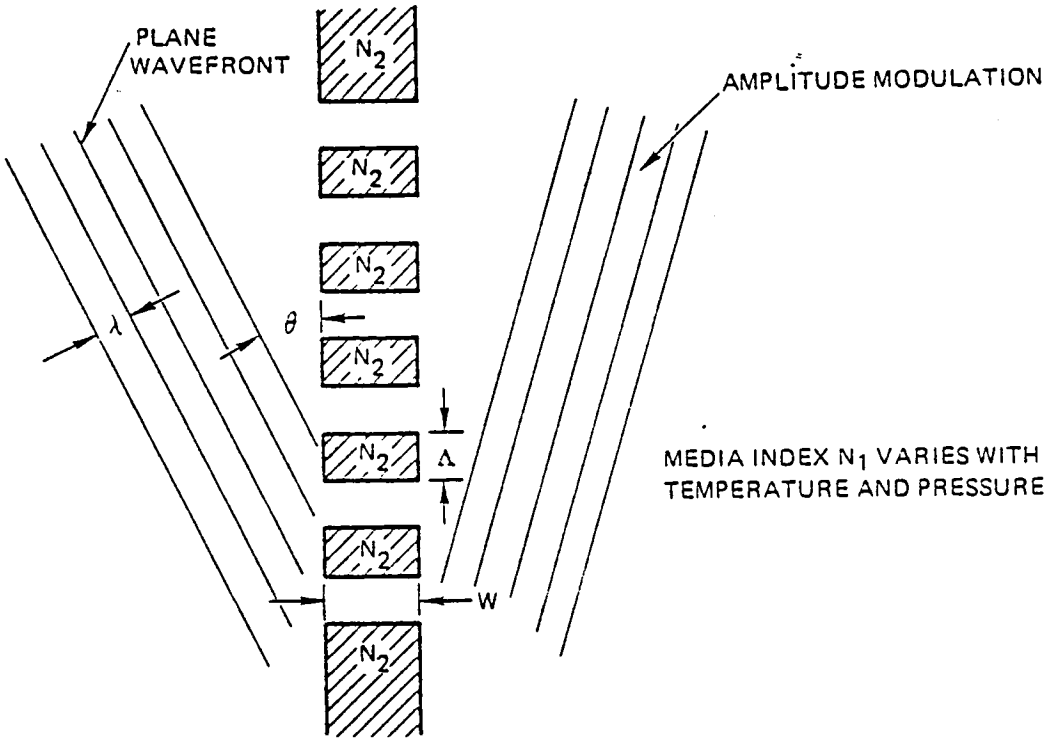

Figure 2.2.9.-1. Bragg Deflector Designed for Sensing Δn Variation.

2.2.10 Conversion of Mechanical Motion to Digitized Optical Signals

The proposal for this contract (dated June 1977) covered several aspects of the conversion of mechanical motion to digitized optical signals in Sections 2.1.2 through 2.1.2.12 of that document. The use of a Holographic Processor to perform this conversion is discussed in this report in the section on the Holographic Processor (2.2.12),as well as in discussions of applications. Other aspects of mechanical motion conversion are discussed below.

In the area of direct masking to perform the function of converting mechanical motion to Gray-coded digitized signals, where each bit of the digitized signal is represented by the presence or absence of light in a corresponding fiber, Figure 2.2.10-1 illustrates the embodiment which is now preferred. It is a direct outgrowth of the principles discussed in the proposal; e.g., a compromise is generally required between sharpness of transition of the individual bits on one hand, and maximum light energy transfer on the other hand. In Figure 2.2.10-1(b), the series of circles represents a group of fiber ends. The mask in Figure 2.2.10-1(b), Mask 1, is permanently attached to the fiber ends. This mask, in addition to providing the functions described below, provides a reference for aligning and checking the alignment of the individual fibers.

In Figure 2.2.10-1(c), the opposing mask, Mask 2, is illustrated. When the two centerlines (dash-dotted lines) are coincident, the output signal is gray-coded 00000, because all open or clear portions of Mask 1 are covered by opaque portions of Mask 2. As Mask 2 moves up, relative to Mask 1, the light intensity in the individual fibers changes as indicated in Figure 2.2.10-1(a). The transitions between dark and light must be assumed to occur at half intensity. It can be shown that the given pattern produces a gray-coded binary which increments each 1/16 inch, to the scale plotted.

The masking is characterized by two types--(1) those portions on the left (the least significant bits) where multiple bars of each mask work against each other, and (2) those on the right (the most significant bits) where one opening in Mask 1 works against a larger pattern in Mask 2.

The advantages of dividing the masking in this fashion are as follows. (1) The multiple masks for the least significant bits provide adequate illumination in the case where the signal must change rapidly and a signal slit would provide only dim illumination. (2) The single slit for the most significant bits produces sufficiently rapid change, at the point of transition from 0 to 1, so that errors are not introduced. Note the third and fourth trace on the right in Figure 2.2.10-1(a): The rate of change of light intensity with position has a minimum rate. In the third, fourth, and fifth trace, the rates of change of intensity with position are the same. (3) For all fibers, the minimum coverage of the fibers is about 50 percent. Thus, the peak light intensity is the same for all bits.

It is believed that this general arrangement is a good choice for direct mechanical masking to produce one bit of information in each fiber.

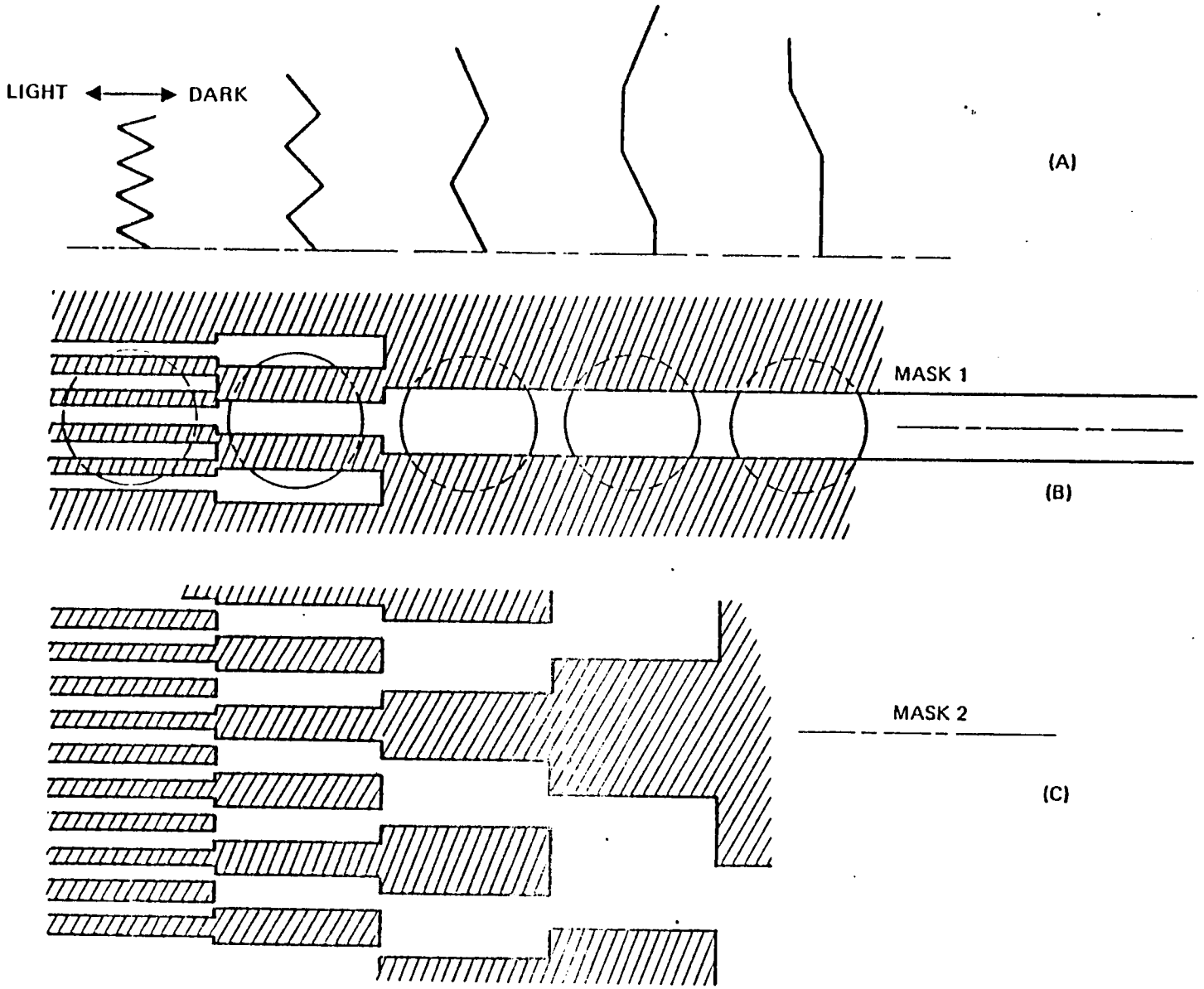

Figure 2.2.10-1. Mask Pair for Fiber-Optic Sensor Gray Coding.

2.2.11 Color Multiplexing

A distinction will be made in this section between color modulation and color multiplexing, although it is clear that there will inevitably be overlapping of the two concepts. The term color multiplexing is used in other fields of fiber optics to indicate that the color, or optical frequency, functions much like a carrier frequently in electrical transmission and that the signals sent over different colors are entirely independent. As used here, the term color multiplexing will refer to separate signals being sent on different carrier colors, but in this application each carrier frequency, or color, will represent one bit of information of a binary word. An example of color multiplexing of this form is shown in Figure 2.2.11-1(b). Here, a white source of light is transmitted from the processor to the remote sensor. At the remote sensor, the light is passed through a prism which breaks the light up into the spectral colors. This light is then focused on a slit behind which is a binary coded mask. As depicted in Figure 2.2.11-1(b), the mask is of the gray coded binary system. This system has been described elsewhere, including the proposal submitted for this program; it has the advantage of never producing a digital signal error which is any greater than the positional error causing the deviation. In Figure 2.2.11-1(b), it is seen that this Gray code mask operates behind the slit which, as stated, is illuminated by spectrally dispersed colors. Thus, as the mask moves, the patterns of color represent the binary bits, which indicates the position of the mask. In this example, red represents the most significant bit and blue the least significant bit. The plot of wavelength distribution shows the binary number 1011. The entire signal is fed along one fiber, or it may be fed along an incoherent bundle if preferred. At the processor, the signal is again broken into its spectrum by the use of a prism, with each color illuminating a suitable photocell. The electrical pattern out of this photocell array is, thus, directly a binary signal--in this case, Gray coded, which indicates the position of the mask. In this case, the mask may be driven by a bimetallic strip to sense temperature, by a bellows to sense pressure, etc.

Two basic features of this system are (1) that it requires only one fiber for the light source and one fiber for the signal being returned, and (2) that the signal output is immediately in a binary coded format, suitable for digital control processing. It should be mentioned that conversion from Gray code to conventional binary is a very simple process. The coded mask could, of course, be designed for conventional binary coding, but with a sacrifice of accuracy, due to the larger potential errors which may result from inconsistent switching time between the various binary bits.

Figure 2.2.11-1(c) shows several variations on the scheme described in Figure 2.2.11-1(b). Again, illumination is by a white source of light; and again, both illumination and signal feedback are on single fibers, or if preferred, on incoherent bundles. Also, the signal being fed back is again color multiplexed. In this case, the color is generated by simply a conventional color filter. This may be any of many types of conventional filters, such as those produced by dies, or it may be an interference-type multiple-layer filter. The Gray-coded binary mask is used in the same fashion as in Figure 2.2.11-1(b).

In Figure 2.2.11-1(c), the color multiplexed signal is decoded onto the individual photosensors by a hologram, rather than by the use of a dispersing prism, as in Figure 2.2.11-1(b). The hologram can work in this fashion because

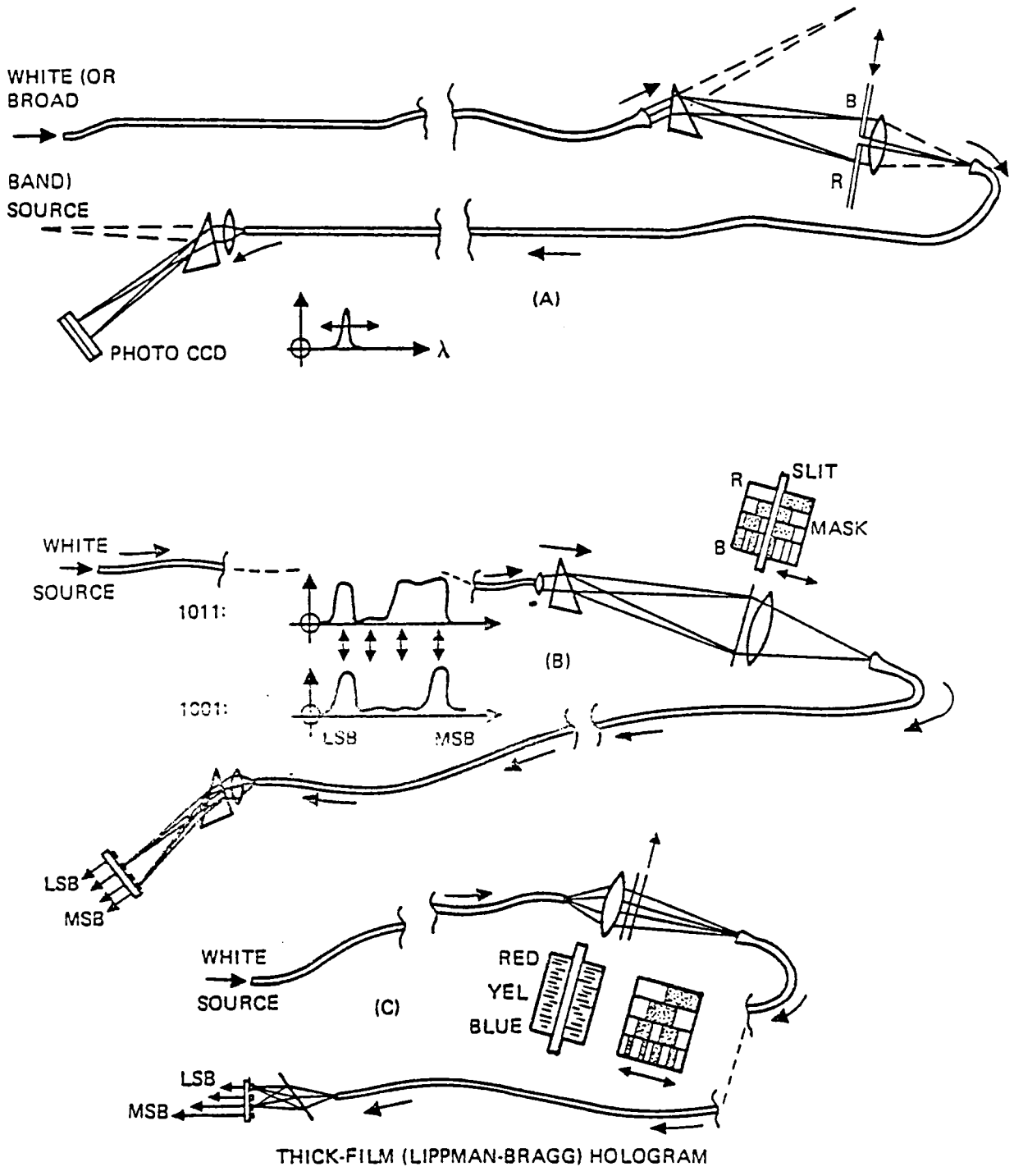

Figure 2.2.11-1. Color Modulation (a) and Multiplexing (b) and (c)

the focus of a hologram is strongly dependent upon the wavelength of the light used. For example, if the blue light focuses to the least significant bit, LSB, then the portion of the hologram which causes this focusing will not cause focusing of light of a longer wavelength. Other components of the hologram will cause other colors to focus at other photosensors, thus creating the desired signal from the set of photosensors. A thick-film (Lippman-Bragg) hologram will aid in this separation of colors, because of the variation of its pattern separation throughout the thickness of the hologram, depending on the wavelength of the light.

Another method of encoding color multiplex signals is represented partially in Figure 2.2.11-2. It is assumed that the input temperature, pressure, etc., causes a white light source to move in the source plane at the left of Figure 2.2.11-2. A and B represent two out of the many points at which this point of light may reside. The hologram in this case is designed so that it always produces an image at the same point in the image plane; namely, the point at which the signal transmitting fiber receives its light energy. However, the hologram is designed so that it transmits various colors to this image point, depending on the location of the source illumination. For example, if a source illumination is at A, then, in this example, blue light only is reinforced at the image point 1. On the other hand, if the light illuminates a source plane at point B, then the hologram will reinforce waves at the image point 1 for both blue and green light. In this fashion, the hologram is designed to convert white light signals along the source plane to color multiplex signals in the output fiber. The hologram of Figure 2.2.11-2 becomes a part of a remote sensor.

It will be noted that Figure 2.2.11-1(b), (c) and Figure 2.2.11-2 all involve, or at least can involve, the identical definition of a color multiplexed signal. Hence, for these various schemes, the white light source, the remote sensor, or the color multiplex decoder at the controller can be interchangeable between the different systems. Another scheme for decoding this basic signal is rather apparent and seems to need no drawing for its description: this scheme is to simply illuminate all photosensors with the returned light, interposing in each case a color filter of conventional design between the signal light and the photosensor. It is also possible for a color multiplex filter mask to be designed so as to compensate for variations in sensor sensitivity variations with color. This is illustrated in Figure 2.2.11-3, where the basic sensor element is illustrated as a prism which has an index of refraction which is sensitive to changes in the basic quantity sensed; for example, the prism may contain a sample of a high-pressure gas, the density of which is to be measured. This is labeled "any beam bending sensor" in the figure because other solid-state beam bending sensors do exist. For example, a conventional diffraction grating, although not possessing very high sensitivity (the percent change of the nominal angular deflection being approximately equal to the percent change of a physical dimension as a result of the temperature), is an example of another sensor of this class. These sensors may have a characteristic that the amount the beam bends is a function of the wavelength or color of the beam. Figure 2.2.11-3(b) is an enlargement of the color multiplex filter (Gray-code) shown in Figure 2.2.11-3(a). If the sensitivity of the beam bending sensor were not a function of wavelength or color, then this color multiplex filter would be the one indicated to be used. However, if, as is the case for the two sensors just mentioned, the long wavelengths tend to bend more or less than the short wavelengths,

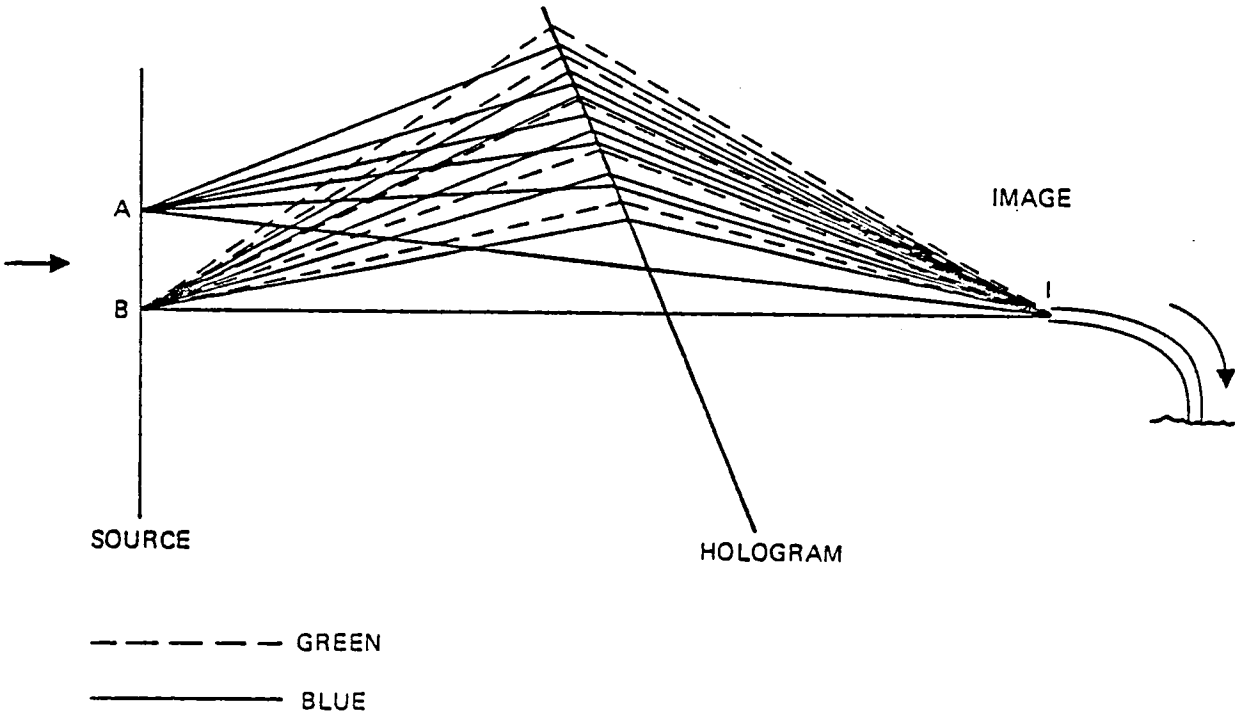

Figure 2.2.11-2. Color Multiplexing With a Holographic Processor.

this effect can be compensated for, as indicated in Figure 2.1.11-3(c) by designing the color multiplex filter mask for different deflections for light beams of different wavelengths or color.

Color Modulation

In contrast to color multiplexing, color modulation is a system where a high-pass, low-pass or bandpass filter changes color or light wavelength in response to the basic sensed signal. This scheme is discussed elsewhere in this report and will be mentioned in this section briefly for contrast to the color multiplexing scheme just discussed. In Figure 2.2.11-1(a), a white or broadband light source is transmitted to the remote sensor, where it is dispersed by means of a prism, a color filter, a diffraction grating, or by other means. In response to the basic sensed input, a portion of this spectrum is allowed to pass through the signal fiber and back to the central processor, where it is analyzed for spectral characteristics. This system is discussed in more detail in another section.

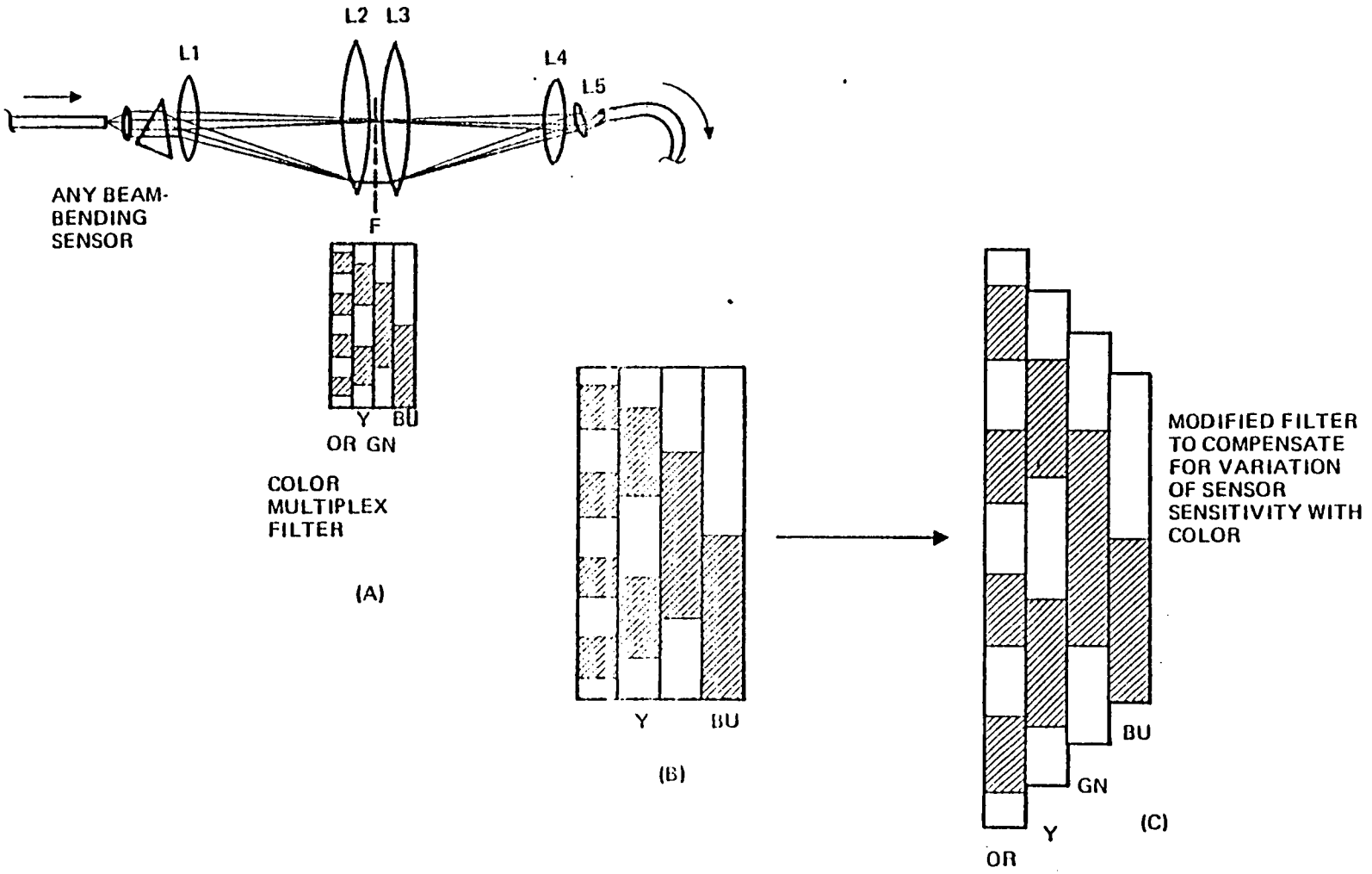

Figure 2.2.11-3. Color Multiplexing and Compensation for Variation in Sensor Sensitivity

2.2.12 Holographic Processor

Introduction

The Holographic Processor is a concept which was developed for application to fiber-optic sensors. The concept has been found to be applicable to a broad range of fiber-optic sensors and is, therefore, being presented in a separate section rather than repeating the concept in discussions of various individual sensors.

The Holographic Processor, in that it transforms a source pattern into an image, appears to have considerable in common with conventional optical information processing systems. In a broad sense, the Holographic Processor is, of course, an optical information processing system. However, the usual optical information processing involves the use of a lens to create a spatial Fourier transform, operates on that Fourier transform--by use of filters, for example--and uses a second lens to recreate the image by performing a Fourier transform. The Holographic Processor as described here has no lenses and involves no Fourier transforms.

In a conventional hologram reconstruction occurs when the hologram is illuminated by a parallel, or spherical, beam of light, normally monochromatic. This light reflects off of the complex pattern of the hologram in a manner so that numerous light rays come into phase at each point in the real image; or, the light may diverge in such a manner that the rays of light appear to have been in phase at points on a virtual image. For example, Figure 2.2.12-3 (although this figure was drawn to illustrate a different point) may be used to describe the operation of a conventional hologram producing a real image. Consider the Source, at the numeral 2, as simply an illuminating monochromatic source for the hologram, H. This drawing then represents the reconstruction by the hologram of just two points of the real image, I, at L$S, and at 2$$. The multiple rays drawn represent, of course, only a small fraction of the thousands of rays which go into the reconstruction of each single point. In a conventional pictorial hologram, the hologram produces, in the manner shown here, all of the points which go into the reconstruction of the real image. The production of a virtual image by a hologram is not illustrated because the Holographic Processor only uses the real image-forming capability of the hologram. (The production of a virtual image is very similar to the production of a real image, except that the beams of light which infer the virtual image diverge from the hologram.)

It will be noted that the holograms in all of the figures in this section are shown aligned at an angle which is not perpendicular to the axis central of the light beams. Calculations,which will be presented later in this section, indicate the importance of tipping the hologram at an angle such as is shown. This tipping was devised as a means of overcoming a type of interference, or crosstalk, which was seen as a potential problem in the desired use of holograms.

Incoherent Bundle to Coherent Signal

Of the many uses to which the holographic processor can be put, in the field of fiber-optic sensors, perhaps the most obvious one is the one depicted in Figure 2.2.12-1. This is the use of the holographic processor for decoding an incoherent linear fiber-optic bundle. Figure 2.2.12-1(a) shows an incoherent

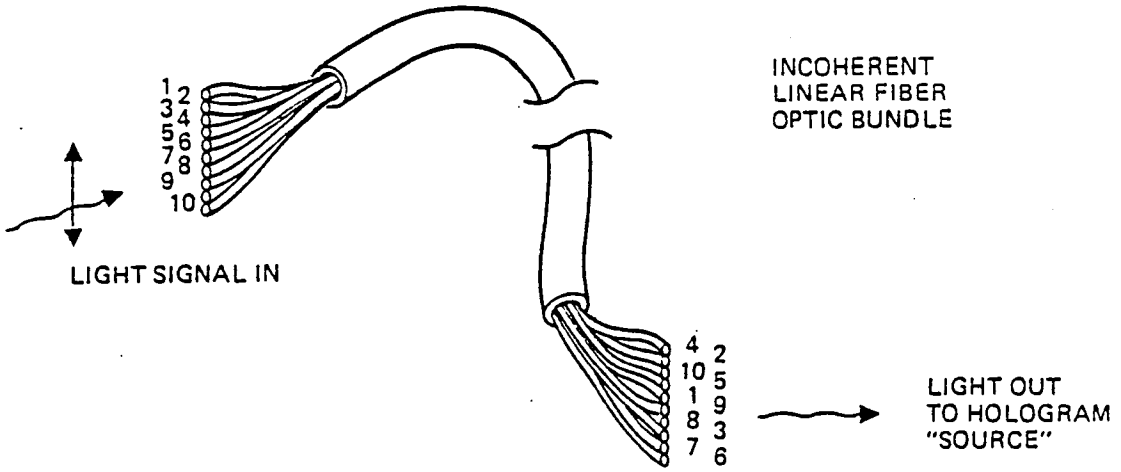

(A)

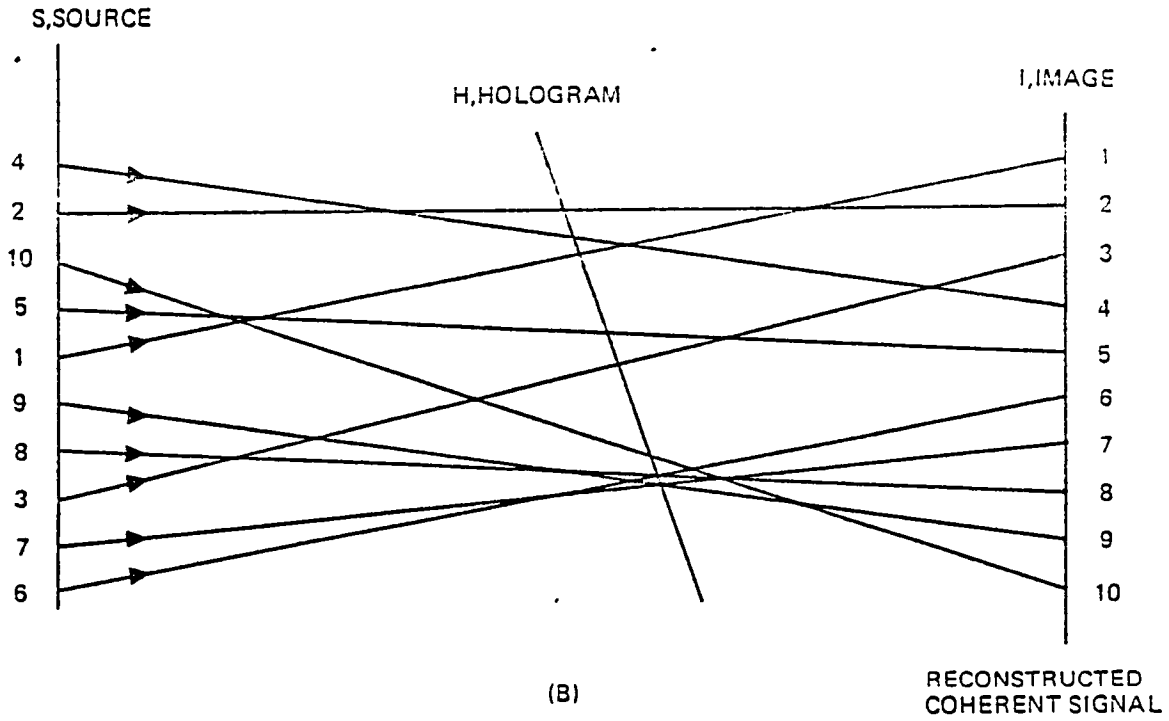

(B)

RECONSTRUCTED
COHERENT SIGNAL

Figure 2.2.12-1. Reconstruction of a Coherent Signal from an Incoherent Signal Using a Holographic Processor.

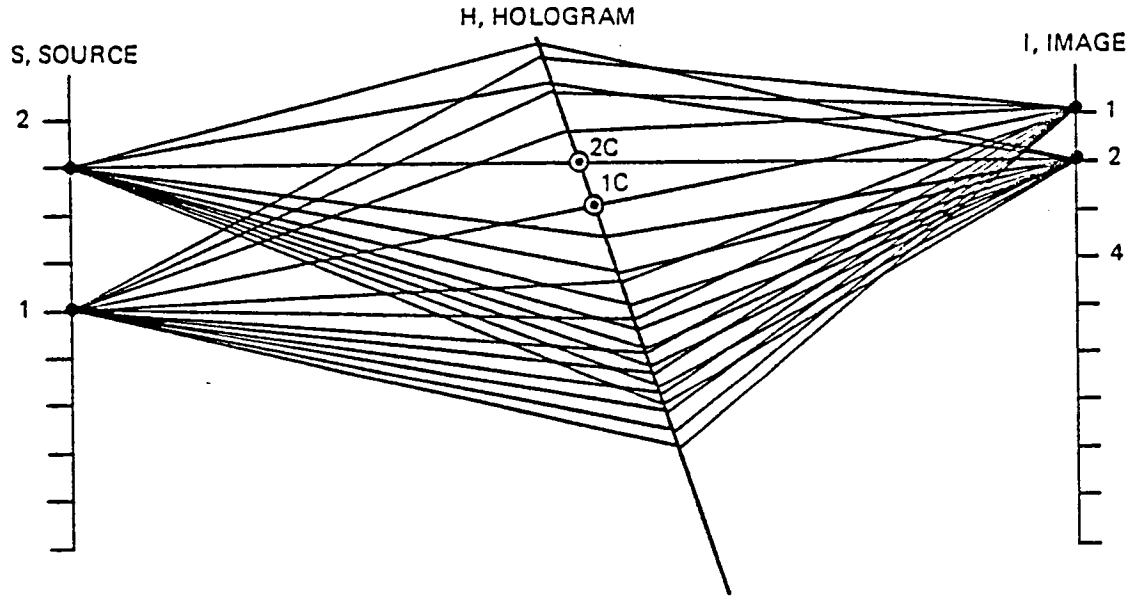

Figure 2.2.12-2. Two Components of a Holographic Processor Designed to Reconstruct a Coherent Signal from an Incoherent Signal.

fiber-optic bundle which has been brought out to a linear array at each end. Because the bundle is incoherent, the location of the fibers at the output end is random with respect to the location of the fibers at the input end of the bundle. This is illustrated by the depiction of ten fibers (a small number used for the ease of illustration). These are numbered directly from 1 to 10 at the input, but with randomly located numbers at the output. The use of a hologram to reorient these signals is depicted in Figure 2.2.12-1(b). The source contains the fiber outputs in the sequence in which they are found to leave the incoherent linear bundle. The hologram then is designed so that, for example, point 4 at the top of source S produces an image only at point 4 in the image plane, which is in the fourth position, as desired. Likewise, each of the other points at the source produces an image at the proper location. The light rays drawn from 4 to 4, from 2 to 2, from 10 to 10, etc., represent only the centerline rays in Figure 2.2.12-1(b). A somewhat more representative set of rays is shown in Figure 2.2.12-2. The rays, for example, which pass from the point 2 in the source to the point 2 in the image are reflected by the pattern in the hologram such that these rays always have path lengths which differ only by integral wavelengths. Thus, the rays, which number in the thousands, are in phase and support each other only at point 2, and in general do not support each other at any other point. The same holds true for the multiple rays from the source point 1, reflecting off of portions of the image in the hologram and forming a supportive image only at the point 1 in the image plane.

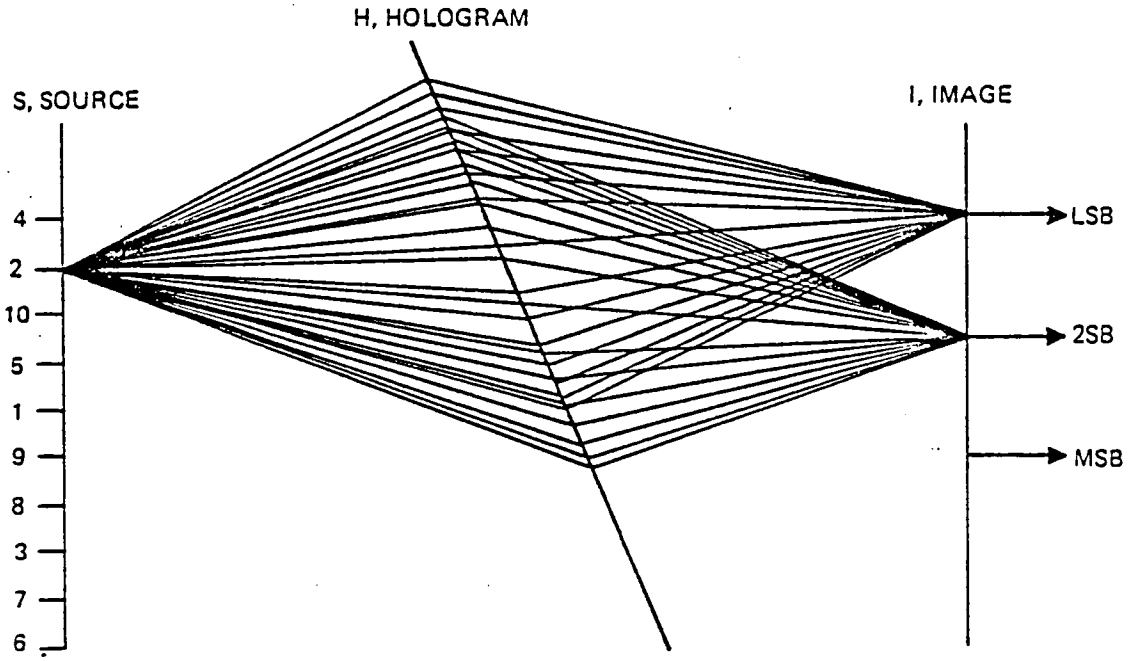

Figure 2.2.12-3. Components of a Holographic Processor Which Images a Source Point into a Binary-Coded Signal

It is noted that the component of the holographic pattern which images any one point into a particular other point, comprises a series of circular patterns which, collectively, are known as a Fresnel Zone Plate. For example, the Fresnel Zone Plate which images source point 1 to image point 1 consists of a set of quasi-circular rings centered about the point 1C. It is apparent then that this pattern consists of the equivalent of a lens with a center at the point 1C, for, as is well known, the Fresnel Zone Plate operates as a lens. The natural question that then arises is: To what extent does the component of the hologram which consists of the Fresnel Zone Plane 1C cause the point 2 in the source to produce an image at the point 4? If this tendency is strong, the entire operation of the holographic image processor could be defeated because, in addition to producing desired images, a wealth of spurious undesired images might also occur. Early in the development of this idea it was thought that these spurious images might well make the Holographic Processor unworkable. In studying this, however, it was discovered that by tilting the hologram, as is shown, it is possible to cause these spurious images to defocus very quickly, even for points quite close to the point for which the zone plate is designed to function. This will be discussed in more detail below.

Incoherent Bundle to Binary Signal

While the restoration of a coherent signal from an incoherent linear fiber-optic bundle is a fairly straightforward application to the Holographic processor as outlined here, other applications seem even more interesting. For example, in the use of an incoherent linear fiber-optic bundle in a sensor application, the direct coherent optical output signal is not the ultimate objective. In this application, the input to the hologram, which would consist of perhaps several hundred fibers, is a signal in which the particular fiber which is illuminated represents the amount of temperature change, pressure change, etc. The ultimate output signal desired is not one of several hundred signals, but in the usual case would be a binary signal, either Gray-coded or conventional binary, which represents the number of the fiber which is illuminated, and thereby the level of signal being measured. Thus, if is were possible to convert the incoherent light output directly to the binary signal which represents this desired quantity, two steps would have been taken.

Figures 2.2.12-3 and Figures 2.2.12-4 show that this double step appears to be no more difficult than the single coherentizing step described in Figures 2.2.12-1 and 2.2.12-2.

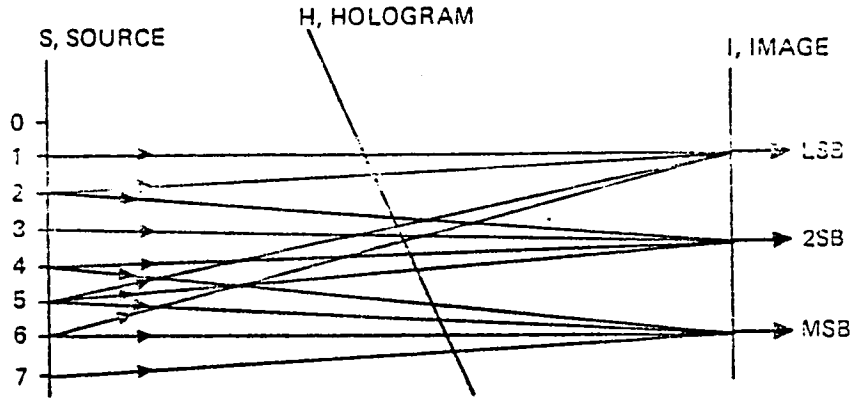

	SIGNIFICANT BITS MOST	2	LEAST
0	0	0	0
1	0	0	1
2	0	1	1
3	0	1	0
4	1	1	0
5	1	1	1
6	1	0	1
7	1	0	0

Figure 2.2.12-4. Centerlines of the Image Rays Which Produce a Gray-Coded Binary Pattern Using a Holographic Processor.

In Figure 2.2.12-3 the point 2 in the source is shown being imaged by the hologram at the two points LSB and 2SB. Thus, the point 2 gives the binary number 011. This number 011 is binary 2 in the Gray-code scheme. This imaging is an exact analog of the conventional use of a hologram to produce a real image; in fact, this figure was used above for purposes of illustrating the conventional holograms. Figure 2.2.12-4 shows the centerline rays for a set of possible source signals, along the paths for which the entire hologram will cause a set of reinforcing waves. Thus, Source 0 produces no image, Source 1 produces an image only at LSB, the least significant bit, Source 2 produces images at LSB and 2SB, etc. These patterns are shown in the chart below to be part of the gray code for the corresponding source numbers.

It is clear that because these relationships between source and image patterns are arbitrary, the binary or Gray-coded binary signals can be produced from either a random source pattern, as in Figure 2.2.12-3, or a sequential pattern, as in Figure 2.2.12-4. In the case of a random source pattern which differs from unit to unit, it will be, of course, necessary to make the holograms individually for each source pattern. When the source is sequential, as in Figure 2.2.12-4, it may be possible to replicate the holograms after making the master hologram by illuminating correspoinding spots on the source and image during the exposure of the hologram. In the case of random source patterns, which will differ from unit to unit, it will be necessary to expose a hologram for each unit individuallly. In either case, this exposure of the hologram is in the same manner as is the normal exposure of holograms.

Figure 2.2.12-5 shows examples of application of the holographic processor of the type which appear the most promising at this time. These represent the use of the hologram as a portion of a remote sensor in a complete fiber-optic system. They enable the fiber-optic sensor to accept a single light source from a fiber, transform this light into a binary or Gray-coded binary signal, and return the coded signal over a small fiber bundle to the central processor. The fiber bundle which carries the return coded signal has only as many fibers as there are bits in the signal (for example, there would be eight fibers and eight bits for a level resolution of one part in 256).

In Figure 2.2.12-5(a) the light beam is shown being sent by a prism. As discussed elsewhere, this prism might consist of a high-pressure gas, sensitive to pressure; it might consist of a solid state refracting material whose index of infraction responds to temperature changes, etc. The beam is then bent according to the sensed input. The position on the source plane S, which is illuminated, through the hologram H, determines which ones of the fibers are illuminated in the image plane I.

In Figure 2.2.12-5(b) the location of the spot of light in the source plane is moved by change of temperature in a bimetallic strip upon which is fastened the end of the illuminating fiber. The hologram again converts the signal to a series of binary or Gray-coded binary signals for transmission back to the central processing unit.

Figure 2.2.12-6 shows the manner in which a group of arbitrary signals at the source plane can be converted to arbitrary binary or Gray-coded binary signals at the image plane. The significance of illustrating the arbitrariness of the conversion which is possible with this scheme is the fact that some

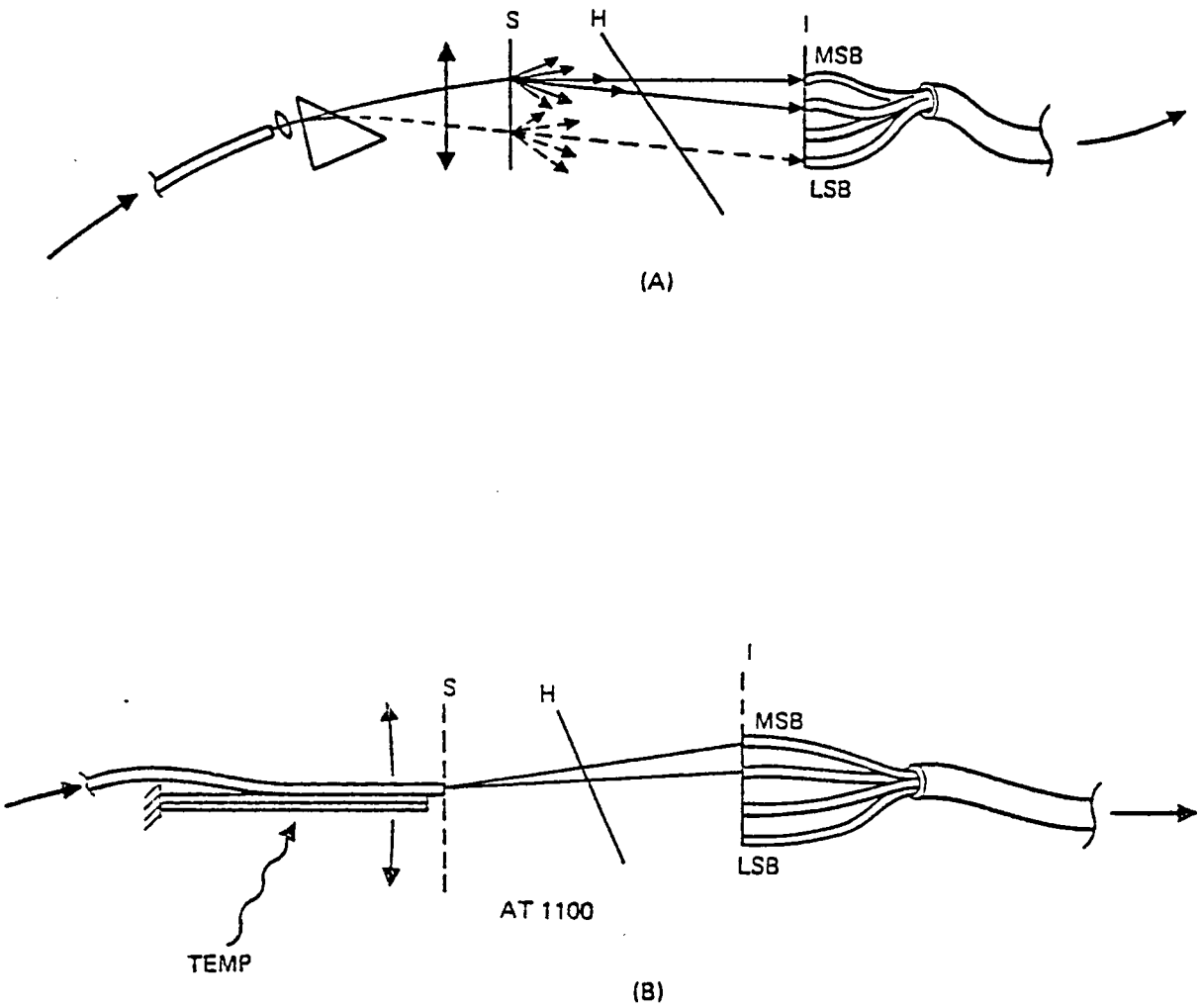

Figure 2.2.12-5. Use of a Holographic Processor to Obtain a Binary Signal From (a) a Beam Deflected by a Variable-Index Prism, (b) Light From the Tip of a Fiber Deflected by a Temperature-Sensitive Bi-Metal Strip.

basic sensors produce rather complex signals in response to the basic input. The holographic processor will permit these signals to be converted directly to a desirable output. The particular source patterns shown in 2.2.12-6 are arbitrary and have no particular significance relative to any particular sensing schemes.

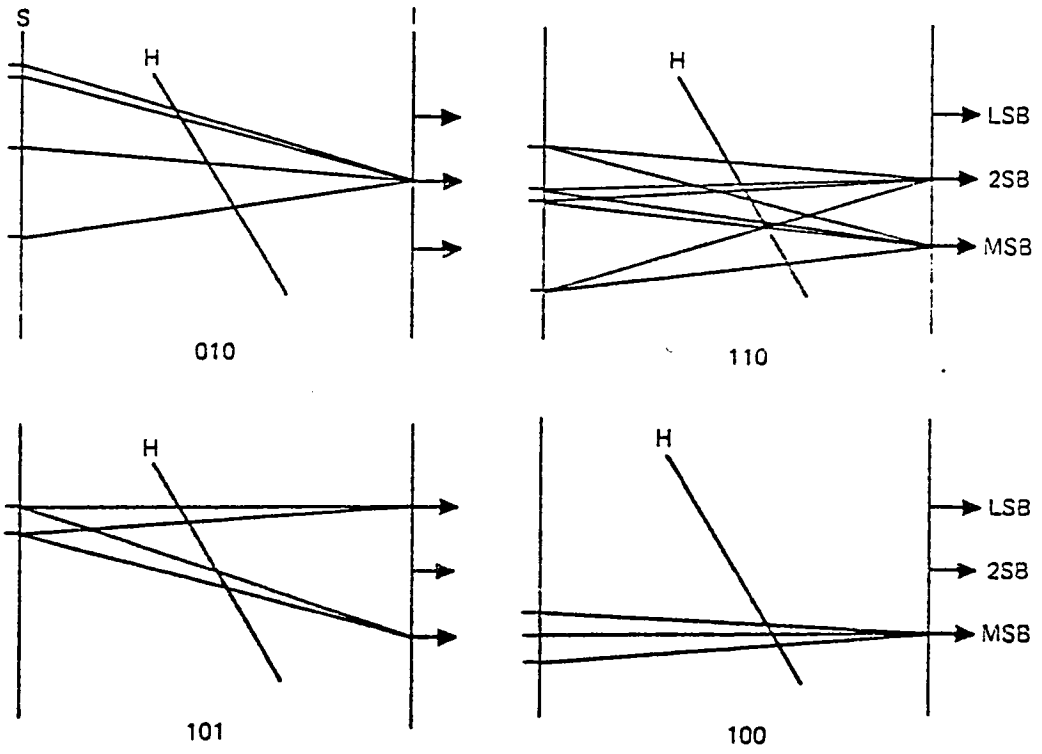

Figure 2.2.12-6. Illustrations of the Ability of the Holographic Processor to Convert Arbitrary Signals to Binary Signals.

Potential Spurious Images: Calculations

The potential problem discussed above in relation to a Fresnel Zone Plate producing spurious images is now investigated. In all three sections of Figure 2.2.12-7, the Source, S, is designed to produce the Image, I. In Figures 2.2.12-7(b) and (c), the source, S' is designed to produce the image, I', the lines between S' and I' not being drawn. Dotted lines, however, are drawn between S' and I''. I'' represents the spurious image that is produced by the component of the hologram which exists for the purpose of producing I from S. This SI Fresnel Zone Plate acts like a lens and possesses the potential capability of producing I'' from S'. In what follows, the degree to which that spurious image is produced will be investigated.

Figure 2.2.12-8 shows some of the quantities used in this calculation. The Hologram, H, will have dispersively reflecting portions at those locations at which the total pathlength from S to W to I exceeds the central pathlength P + Q by an integral number of wavelengths, N. The pathlength from S' to I'' is L1 + L2 = L. If a spurious image at I'' is to be formed, then all of these pathlengths, L, for the various values of W for which the hologram has dispersively reflecting portions, must differ by integral numbers, or nearly integral numbers.

Because this calculation is not amenable to a closed mathematical form, it was handled on a computer in the following manner. For each value of N for which a calculation is to be made, the value of W at which the total pathlength equals P + Q + N is found by iteration. This value of W is then used to find the length of the path from S' to W to I''. The amount by which this pathlength differs from the central pathlength is then calculated as L - LØ. Finally, the amount by which this value differs from the value N is calculated as the amount by which the light ray through that portion of the hologram deviates from being in phase with the central light ray. For reference, the program is attached in Appendix A. Samples of a computer run are reproduced in Figures 2.2.12-9, -10, and -11. Figure 2.2.12-7 is a scale drawing of this computer run. For a wavelength of 7000 Å, this scale drawing is one-quarter inch to 1 millimeter. The increments of Y in this case are about one-tenth millimeter, or 100 microns, which is a reasonable spacing for adjacent fibers in a bundle. In Figure 2.2.12-9, the first run is for theta = 0, and it is seen that the calculations were made at every one-hundredth fringe. It is seen that with theta = 0 and Y = 0 that the quantity N - (CØ) is everywhere 0. This portion of the run actually serves simply as a check on the program because the hologram is being designed at this point for complete support; thus, if these terms were not everywhere 0, there would be an indicated error in the program. For a value of Y of 150 wavelengths (about 100 micrometers) it is seen the N - (CØ) varies from 0 to .278. This indicates that as far out as the nine-hundredth fringe, which is a distance of W = 3033 wavelengths, the phase difference is only one-quarter of a wavelength. Thus, it would be expected that a fairly large spurious signal would occur at this location.

The theory that was intended to be tested by this program is that by tipping the hologram, this spurious signal will be decreased. The results of this tipping are shown in Figure 2.2.12-10. Here, with the value of theta = .4 radians (about 22°), it is seen that the value for N - (CØ) is again everywhere 0 when Y = 0. This again serves as a check because the hologram is designed for this point. The point of major interest, however, are the values for the quantity Y = 150 wavelengths; at this value, it is seen that, as N varies from 0 to 800,

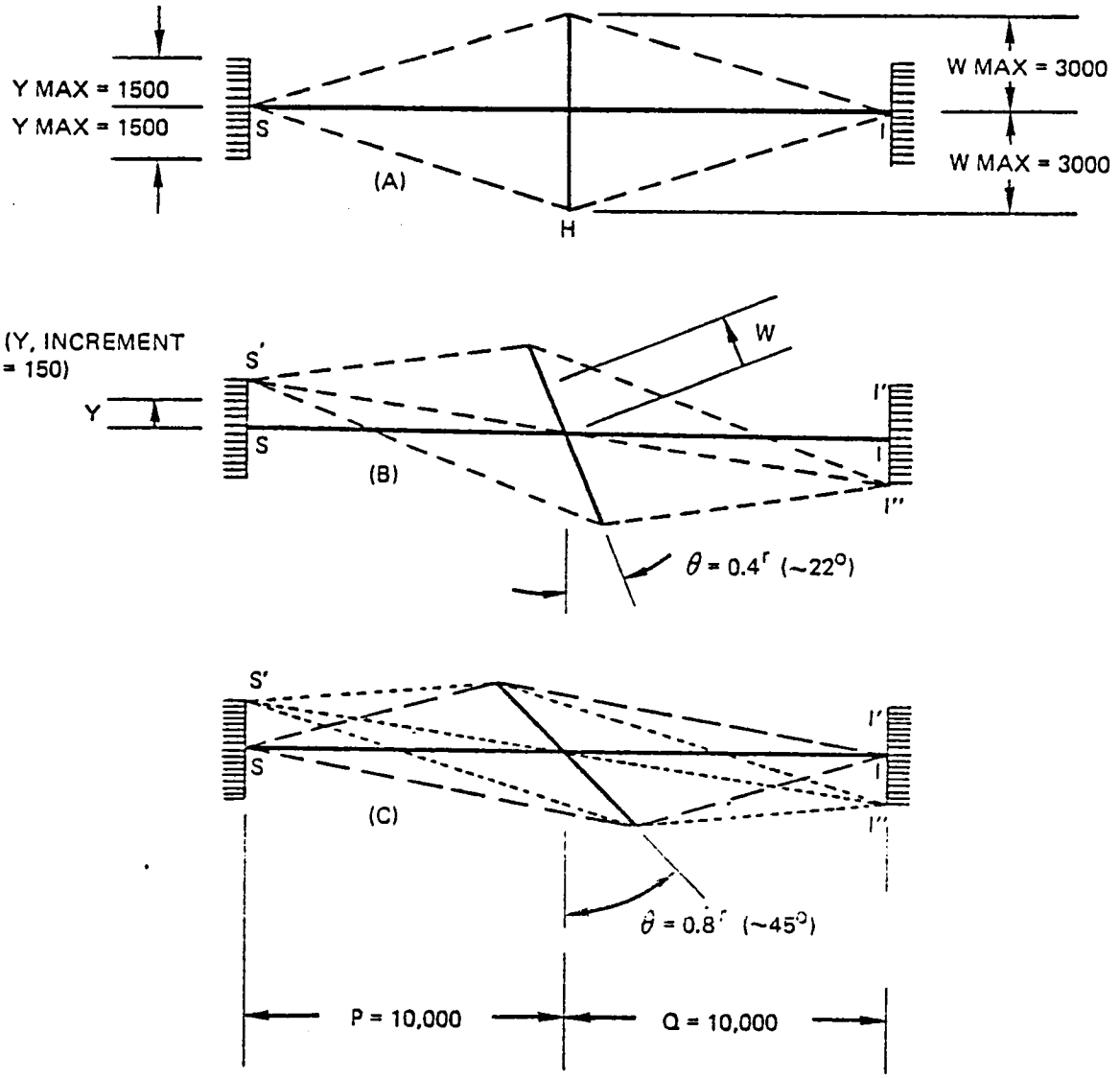

FOR $\lambda = 0.7\,\mu$M, Pλ = Qλ = 7 MM
Yλ MAX = 1.05 MM Yλ INCR = 0.105MM
Wλ MAX = 2.1 MM
SCALE AT $\lambda = 0.7\,\mu$M: ¼ INCH = 1MM (6.35 X)

Figure 2.2.12-7. The Holographic Processor: Scale Drawing for Computer Run of 77-12-22.

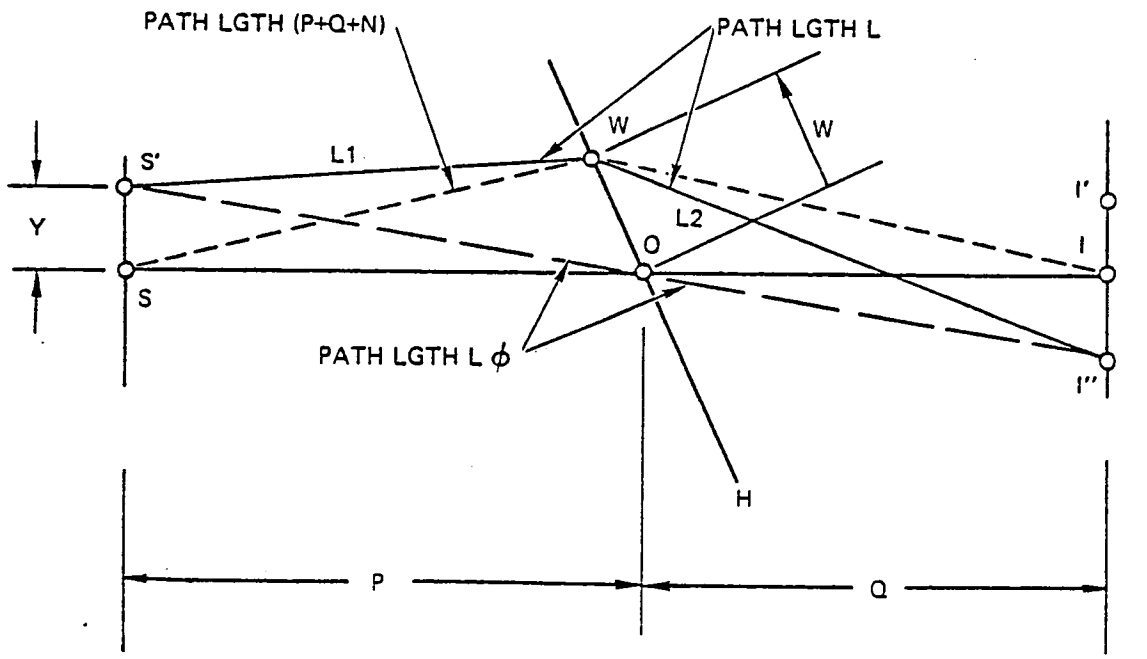

(ALL DISTANCES MEASURED IN NUMBER OF WAVELENGTHS)

$L = L1 + L2$

$C = L - (P + Q)$

$L\phi = L \Big]_{\substack{N=0 \\ W=0}}$

$C\phi = C \Big]_{\substack{N=0 \\ W=0}} = L\phi - (P + Q)$

$L - L\phi = C + (P + Q) - [C\phi + (P + Q)]$

$= C - C\phi$

AT Y=0, THE HOLOGRAM IS DESIGNED SO THAT $(C - C\phi) = (L - L\phi) = N$ FOR ALL N

Figure 2.2.12-8. The Holographic Processor: Definition of Terms Used in Computer Program.

and W varies from 0 to 3080, the value of N - (C - CØ) varies from 0 to 9.42. This represents considerable phase shift. This amount of phase shift would be expected to very nearly eliminate this spurious signal. This represents a very rapid defocussing of the Fresnel Zone Plate because the source has moved only the small distance of 150 wavelengths, or about 100 micrometers. To see the effect of tipping the hologram, we compare the quantity 9.42 in Figure 2.2.12-10 to the quantity .278 in Figure 2.2.12-9.

These results are believed to indicate that a hologram can be used successfully in the various ways in which it is described in this section, and in other similar fashions.

Generation of Holograms

The exposure, or generation, of all of the types of holograms which have been discussed in this section follows the same general procedure. Components of the hologram are generated by sequentially illuminating the hologram from desired pairs of source and image points from a common coherent light source. For example, in Figure 2.2.12-2, source point 1 and image point 1 may first be illuminated, using mirrors and beam splitters, from a common laser beam. Next, source point 2 and image point 2 are simultaneously illuminated. The first exposure forms a component of the hologram which consists of a Fresnel Zone Plate centered about 1C; the second exposure, illuminating the hologram from source point 2 and image point 2 produces a zone plate centered about 2C. The rest of the hologram is built up in this manner, preferably using a mechanized system for indexing the exposures.

More than one component of the hologram can be exposed at one time. This is shown by the fact that a conventional (pictorial) hologram is built up by illuminating, simultaneously, all points in the object and exposing the hologram with the light reflected from this object and, at the same time, with the reference beam. For example, in Figure 2.2.12-3, the source point 2 is intended to produce image points at both LSB and 2SB. Hence, if LSB and 2SB are illuminated simultaneously and coherently with source point 2, the exposure of the hologram will be an exact analog of the exposure of a conventional hologram where source point 2 replaces the reference beam,and LSB and 2SB replace two points of the image.

If the source contains 256 elements and the image contains 8 elements (the 8 bits which represent the number 256), it would appear practical to make the entire hologram with just 8 exposures--exposing each bit simultaneously with all of the source points which contain that bit.

Several other types of holograms which have been conceived are discussed in different sections of this report. For example, in Figure 2.2.11-2, all source points image to the same point in the image plane, but do so with different colors. This is described in that section.

It will be noticed that a feature of the holograms described in this report, which differs from the conventional hologram, is that while there are multiple points in the image, as is true in the conventional hologram, there are also multiple points in the source. The source, in drawing an analogy to a conventional hologram, replaces the reference beam. It is not known whether holograms have been used in just this manner previously, or if so, if a standard terminology has been given to usage of this type. For the present usage,

```
3, 4 (ADD C-C0), OR 5 (ADD D2) OUTPUT COLUMNS?
 ? 3
VALUES OF P,Q
 ? 10000,10000
T MIN,  T MAX,  T INCR
 ? 0,.8,.4
MAXIMUM VALUE OF W
 ? 3000
Y MIN,Y MAX, Y INCR
 ? 0,1500,150
VALUES OF N1,N FINAL,N INCR
 ? 0,2500,100
```

$P = Q = 10,000$

$T(\theta) = 0,\ 0.4,\ 0.8$

$W_{max} = 3000$

$Y = 0, 150, 300, 450, 600, 750$
$900, 1050, 1200, 1350, 1500$

$N = 0, 100, 200, \ldots 2500$ max (unless W max reached first)

```
 N              N-(C-C0)        W
===             ========       ===

****** THETA =  0              ********

VALUE OF Y:     0
VALUE OF C0     9.77516E-6

 0              0               .313639
 100            0              1001.25
 200            0              1417.74
 300            0              1738.53
 400            0              2009.98
 500            0              2250.
 600            0              2467.79
 700            0              2668.8
 800            0              2856.57
 900            0              3033.56

VALUE OF Y:     150
VALUE OF C0     2.24988

 0              0               .313639
 100            .0334          1001.25
 200            .0661          1417.74
 300            .0982          1738.53
 400            .1297          2009.98
 500            .1606          2250.
 600            .1908          2467.79
 700            .2205          2668.8
 800            .2497          2856.57
 900            .2782          3033.56

VALUE OF Y:     300
VALUE OF C0     8.99799

 0              0               .313639
 100            .1335          1001.25
 200            .2644          1417.74
 300            .3927          1738.53
 400            .5185          2009.98
 500            .6419          2250.
 600            .7629          2467.79
 700            .8816          2668.8
 800            .998           2856.57
 900            1.1122         3033.56
```

Figure 2.2.12-9. Holographic Processor Calculations--Computer Run Portion 1

```
THETA = 0, CONT:
VALUE OF Y:       1500
VALUE OF C0       223.748

 0                3                .313639
 100              3.2514           1301.25
 200              6.4415           1417.74
 300              9.5718           1738.53
 400              12.6436          2009.98
 500              15.6581          2250.
 600              18.6168          2467.79
 700              21.5238          2668.8
 800              24.3713          2856.57
 900              27.1696          3033.56


****** THETA =  .4                ********

VALUE OF Y:       0
VALUE OF C0       8.16584E-6

 0                0                .314118
 100              0                1086.1
 200              0                1536.55
 300              0                1882.6
 400              0                2174.7
 500              0                2432.38
 600              0                2665.65
 700              0                2880.46
 800              0                3080.69

VALUE OF Y:       150
VALUE OF C0       2.24988

 0                0                .314118
 100              1.2819           1086.1
 200              2.5327           1536.55
 300              3.7531           1882.6
 400              4.9437           2174.7
 500              6.1053           2432.38
 600              7.2385           2665.65
 700              8.3438           2880.46
 800              9.422            3080.69

VALUE OF Y:       300
VALUE OF C0       8.99798

 0                0                .314118
 100              2.6235           1086.1
 200              5.1789           1536.55
 300              7.6763           1882.6
 400              10.114           2174.7
 500              12.4934          2432.38
 600              14.8156          2665.65
 700              17.0819          2883.46
 800              19.2935          3083.69
```

Figure 2.2.12-10. Holographic Processor Calculations--Computer Run Portion 2

```
 ..... THETA =  .8

VALUE OF Y:      0
VALUE OF C0      4.58956E-6

 0               0               .314573
 100             0               1429.62
 200             0               2014.
 300             0               2457.44
 400             0               2827.36
 500             0               3150.02

VALUE OF Y:      150
VALUE OF C0      2.24988

 0               0               .314573
 100             3.0635          1429.62
 200             6.0467          2014.
 300             8.9586          2457.44
 400             11.7967         2827.36
 500             14.5611         3150.02

VALUE OF Y:      300
VALUE OF C0      8.99798

 0               0               .314573
 [illegible]     [illegible]     [illegible]
 [illegible]     12.[illegible]  [illegible]
 600             17.9822         2457.44
 400             23.6897         2827.36
 500             29.2546         3150.02

VALUE OF Y:      450
VALUE OF C0      20.2398

 0               0               .314573
 100             9.2244          1429.62
 200             18.2421         2014.
 300             27.0524         2457.44
 400             35.6554         2827.36
 500             44.0512         3150.02

VALUE OF Y:      600
VALUE OF C0      35.9677

 0               0               .314573
 100             12.3154         1429.62
 200             24.3662         2014.
 300             36.1512         2457.44
 400             47.6696         2827.36
 500             58.9212         3150.02

VALUE OF Y:      750
VALUE OF C0      56.1711

 0               0               .314573
 100             15.4041         1429.62
 200             30.4916         2014.
 300             45.2682         2457.44
 400             59.7083         2827.36
 500             73.8349         3150.02
```

Figure 2.2.12-11. Holographic Processor Calculations--Computer Run Portion 3

the term "Holographic Processor" has been assigned to uses of the hologram where the source, which replaces the reference beam in a conventional hologram, becomes a variable in location, or may have multiple values of location at a given moment.

2.2.13 Semiconductor Variable-Band-Gap Filter for Color Modulation of Point Source Motion

Consider a moving point source of broad-band illumination. The movement might be due to the mechanical motion of a fiber terminus or the solid state deflection of a Bragg cell. If the illumination were to impinge on a graded filter--one with cutoff wavelength varying linearly with position over the filter length (high-, low-, or band-pass)--the position of the light source could be transmitted via color modulation (Figure 2.2.12-1). As the point source illumination moves across the graded filter it encounters different filtering characteristics and the resultant filtered spectrum indicates the section on the filter which is being illuminated. This spectral information can be deciphered by a color modulation/detection subsystem.

A simple and efficient graded filter can be fabricated by growing graded band-gap semiconductor crystals or by depositing amorphous semiconductor films of varying composition. Such a graded filter can be made to operate in the manner discussed in Section 2.2.4.

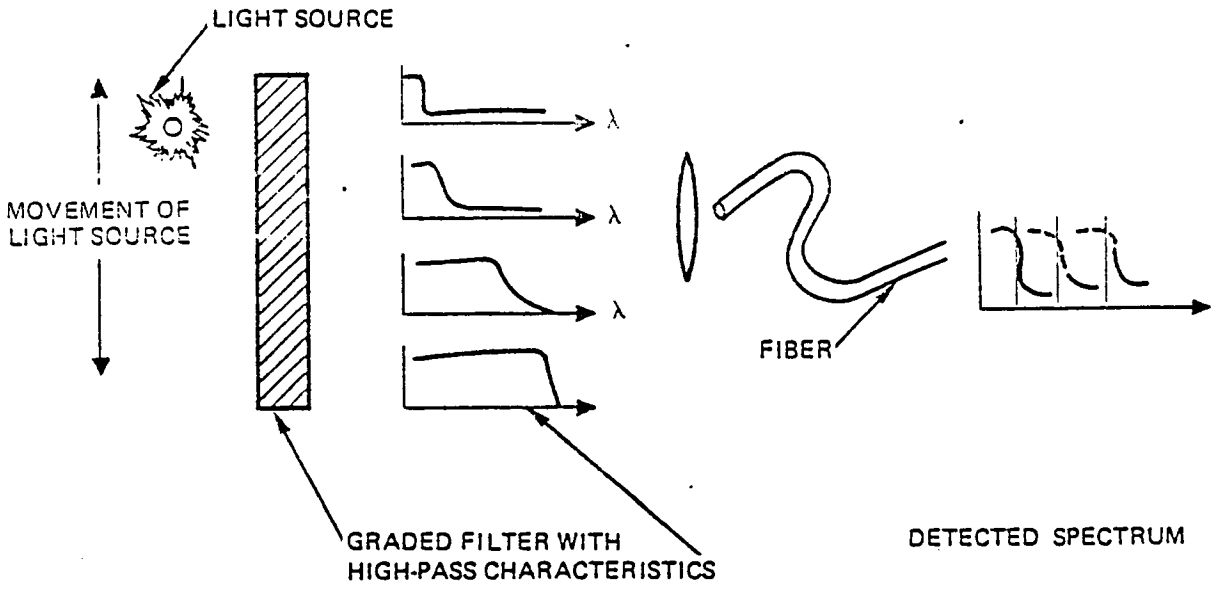

Figure 2.2.13-1. Graded High Pass Filter Used in Color Modulation of Point Source Position

2.3 DETECTION SUBSYSTEM

Detector subsystems have not been studied under this contract, except as required to evaluate particular sensor concepts. However, in some cases, an element developed for use in sensing may also be useful as a detector.

2.3.1 Binary Modulation Detection. In binary modulation, as defined here (including Gray code), each bit of information is carried in a separate fiber. Thus, if a signal has 1024 levels, the binary modulated signal would be carried in a coherent bundle of just ten fibers. Detection in this case is straightforward. One photodetector per fiber generates one bit of electrical information, which may be fed into an electrical processor circuit in any manner required.

2.3.2 Pulse Width Modulation Detection. The measurement of pulse widths by gated counters, etc., is also straightforward, once the optical signal has been converted to an electrical pulse. The concept of pulse width detection has been extended somewhat in Section 2.2.2 to include the exponential-decay pulses generated by a luminescent temperature detector. In this case, the exact beginning and end of the pulse must be accurately defined for proper sensor operation (see Section 2.2.2).

2.3.3 Pulse Frequency Modulation Detection. Pulse frequency modulation consists of a detection subsystem which samples the optical signal for a given length of time and counts the number of incoming pulses during that period. This count--which is proportional to frequency--is converted to an electrical signal compatible with digital electronics.

2.3.4 Color Modulation and Color Multiplexing Detection. Color modulation has been defined to include shifts in band-pass wavelength and shifts in high- or low-pass wavelengths, as well as shifts in the spectra of more complex patterns (as in multiple-beam interference sensors at the larger gaps). These frequencies, or colors, may be separated by a prism or a grating, onto a photosensor array, and the electrical output analyzed for the spectral characteristics.

A more interesting method of analyzing such spectra is the use of what is termed here, a Holographic Processor. This device, initially visualized for use in remote sensors, also indicates potential for use in the detection of complex signals, such as color modulated signals. As discussed in detail under the Holographic Processor (2.2.12) and also under individual applications, this device offers promise for converting complex color-modulated signals directly to binary outputs.

Color multiplexing, the term used here for binary signals where each bit is coded as the presence or absence of light of a particular wavelength or color, has basically the same requirements for sensing, and the above comments generally apply. In the case of dispersion by prism, however, a smaller photosensor array may be used since only one sensor is required for each binary bit. Also, because of the smaller number of color bands or channels, it is possible, in the case of color multiplexing, to separate the individual color signals at the photosensors, using conventional color filters only.

2.3.5 Holographic Processor--Incoherent to Coherent Bundle. The holographic processor, in addition to several uses in sensors, shows promise for use as a processing element for decoding a linear array of fiber outputs of an incoherent bundle. This application is described in the discussion of the holographic processor, Section 2.2.13

3.0 RESULTS AND DISCUSSION

Various fiber-optic sensors were investigated. The study was restricted to those sensors which both receive light for excitation through an optical fiber and transmit the signal, a measure of the sensed quantity, back to a central processor through an optical fiber.

In many of the sensors analyzed, the complete sensor consists of two elements. The first element converts the quantity being sensed to some intermediate quantity, while the second converts the intermediate quantity to a form suitable for transmission. In these cases, each element is a sensor component and,frequently, these elements can be paired to form more combinations than there are individual elements.

A series of birefringent crystals, with a polarizer and analyzer at the ends of each, can be used to produce the binary bits of a coded temperature signal. The sensitivity would be very good, but a problem exists in the lack of sharp transition between the "off" and the "on" state in the case of the more significant bits.

The pulse-width modulated luminescent sensor is, in construction, the simplest sensor considered. It uses the same fiber for both driving the sensor and for returning the signal. The sensor consists simply of a spherically terminated end which has been coated with a phosphorescent material. Because the decay rate of phosphors are a strong function of temperature, the time required for the phosphorescent illumination to decay to a fixed ratio of the initial value is a pulse width which is a function of temperature. The measurement of the ratio of light intensities during decay permits pulse widths to be measured without interference caused by variation in attenuation of the signal-transmitting fiber.

A luminescent temperature detector of the construction just described can be used to sense temperature by means of utilizing the shift in wavelength, or color, of the phosphorescent return signal. The sensor, the optical drive, and the transmitting fibers are identical. Only the quantity sensed, the detector, and the choice of phosphorescent material are different.

The temperature (and/or) pressure-dependent semiconductor filter provides a color-modulated signal which is characterized by high-pass cutoff wavelength. The prime advantage of this type sensor is ease of fabrication. Using crystalline material requres a straightforward sandwiching of optical materials. Using amorphous materials, however, allows for one of many simple thin-film deposition techniques to be performed.

The use of coupled polarized modes provides a means of forming a band-pass filter using only an inherent material property rather than a microfabricated structure. Color-modulation techniques in a coupled polarized mode filter can be made more sensitive by using a band-pass rather than a high-pass or low-pass filter. This is due to a peak wavelength being more easily defined by electronic processing than a somewhat gradual cutoff wavelength.

The Raman-Nath and Bragg sensors provide light patterns sensitive to temperature, pressure, or gas density. The sensitivity, however, is not as high as would be desirable. The sensitivity corresponds to that of a conventional diffraction grating which senses temperature changes by its change in ruling spacing with temperature. This means an optical lever is required to obtain reasonable sensitivity.

Numerous methods exist for converting mechanical motion to digitized optical signals. In addition to Holographic Processor applications, discussed below, numerous mask or multiple shutter schemes are practical. The preferred scheme has the advantages of sharp transition of the most significant bits, adequate light on the least significant bits, high sensitivity to small motions, a fiber mask which aids in fiber alignment and check thereof, and the error limitations inherent in the Gray code.

"Color Multiplexing," is often associated with transmission; however, here it serves as a focal point for several of the sensor concepts. The term is used here to refer to transmissions in which each bit of binary (conventional or--preferrably--Gray code) information is carried by a particular color, or wavelength.

The first element of a color-multiplex sensor is one which produces in some way, a changing light pattern or a mechanical motion. This includes solid-state sensor elements which bend a beam, such as a diffraction grating, or a prism of variable index of refraction, and mechanically actuated mirrors or fiber ends. Generally, color modulating sensors would not be included as such a first element, because they produce signals suitable for transmission without further conditioning.

In the case of a mechanical motion, the illuminating light is broken into a spectrum by a prism or by a color filter, and the mechanical motion drives a coded mask. In the case of a bent beam, the beam may pass through a suitable mask, or, as described below, a Holographic Processor may be used to transcribe the changing light pattern into a color-multiplexed signal.

All of these color-multiplexed schemes have the advantage of providing a signal which is independent of fiber attenuation, requires only one fiber for transmitting the entire coded signal, and provides a signal which is already digitally encoded.

The Holographic Processor is not an entire sensor, but one of the elements of a sensor. The element which precedes the Holographic Processor in a sensor is a device which modifies a light beam in some manner. By suitable construction, the Holographic Processor is able to process this beam into any transmission code chosen, out of a large number available--the most important of which are the coherent-bundle-binary (one fiber per bit), and the color-multiplexed (as just described) signals.

The Holographic Processor also has promise for use as a decoder at the processor. For example, a Holographic Processor could be used to color-multiplex a signal at the sensor, then a second Holographic Processor could be used at the detector to decode the color-multiplexed signal into a binary pattern onto a set of photodetectors.

4.0 CONCLUSIONS AND RECOMMENDATIONS

This report considers twenty fiber-optic sensor subsystems. Depending on application requirements, various combinations of these subsystems can be used to form a sensor system with a digital transmission format which is unaffected by power interruptions, etc. The subsystems are divided into three groups--light source, sensor and detector--as follows:

A. Light Source

1) Narrowband
2) Broadband

B. Sensors

1) Birefringent crystal
2) Pulse-width luminescent
3) Wavelength luminescent
4) Semiconductor filter
5) Coupled polarized mode
6) Multiple-beam interference
7) Vibration frequency modulation
8) Raman-Nath
9) Bragg
10) Mechanical digitized mask
11) Color multiplex
12) Holographic Processor
13) Semiconductor bandgap

C. Detector

1) Digital amplitude
2) Pulse width
3) Pulse frequency
4) Spectral analysis
5) Holographic Processor

All these subsystems, and the systems which are obtained by combining them, have certain desirable features and advantages. At least three of these systems are not only extremely promising, but are diverse enough in concept to make a further study a very difficult task. The authors have converged on these three systems for further study because they embody the key principles involved in the concepts used for all of the above-listed subsystems. These three systems are as follows:

A. Interference filter with temperature-dependent geometry utilizing color modulation.

B. Luminescent material with dependent emission decay time utilizing pulse-width modulation.

C. Point source of light with pressure-dependent motion utilizing a Holographic Processor to convert motion to color multiplex.

5.0 REFERENCES

1. Anderson, W. J., et al: "Optical Rotatory Dispersion of $AgGaS_2$," Opt. Comm., Vol. 11, August 1974.

2. Arecchi, F. T. and Schultz-Dubois, E. O., Editors: Laser Handbook, Vol. 2, North-Holland Publishing Co., Amsterdam, 1972.

3. Arnaud, J. A.: Beam and Fiber Optics, Academic Press, New York 1976

4. Baranets, I. V., et al: "Oscillator Strengths for Excitons in CdS Using the Rozhdestvenskii Hook Method," Opt. Sepctrosc., Vol. 37, August 1974.

5. Born, M. and Wolk, E.: Principles of Optics, Pergamon Press, London, 1959.

6. Bradley, CC.: High Pressure Methods In Solid-State Research, Plenum Publishing, New York, 1969.

7. Collins, R. E.: Field Theory of Guided Waves, McGraw-Hill, New York, 1960.

8. Curie, D.: Luminescence in Crystals, 2nd ed., Methuen and Co., Ltd., London, 1963.

9. Dakss, M. L., et al: "Holographic Grating Analysis," Appl. Phys. Lett., Vol. 16, 1970.

10. Den Hartog, J. P.: Mechanical Vibrations, 3rd ed., McGraw-Hill, New York, 1947.

11. Fowles, R.: Introduction to Modern Optics, Holt, Rinehart & Winston, New York, 1968.

12. Franson, M.: Modern Applications of Physical Optics, John Wiley & Sons, New York, 1963.

13. Gagliardi, R. M. and Karp, S.: Optical Communications, John Wiley & Sons, New York, 1976.

14. Goldberg, P., Editor: Luminescence of Inorganic Solids, Academic Press, New York, 1966.

15. Harris, L. and Siegel, B. M.: "A Method for Evaporation of Alloys," J. Appl. Phys., Vol. 19, August 1948.

16. Henry, C. H.: "Coupling of Electromagnetic Waves in CdS," Phys. Rev., Vol. 143, March 1966.

17. Hodara, H., Editor: Fibers and Integrated Optics, Proc. of the Soc. of Photo-Optical Instr. Engr., Vol. 77, SPIE, Palos Verdes, California, 1976.

18. Hungarian Academy of Sciences, Roland Eötvös Physical Society: International Symposium of Luminescence, Akadémiai Kiadó, Budapest, 1962.

19. Igo, T. and Toyoshima: "A Reversible Optical Change in the As-Se-Ge Glass," J. Non Crys. Sol., Vol. 11, 1973.

20. Jenkins, F. A. and White, H. E.: Fundamentals of Optics, 3rd ed., McGraw-Hill, New York, 1957.

21. Laurenti, J. P., et al: "Optical Filters Using Coupled Light Waves in Mixed Crystals," Appl. Phys. Lett., Vol. 28, February 1976.

22. Lean, E. G. H.: Progress in Optics, XI, Editor E. Wolf, 1973

23. Leverenz, H. W.: An Introduction to Luminescence of Solids, John Wiley & Sons, New York, 1950.

24. Levi, L.: Applied Optics, Vol. 1, John Wiley & Sons, New York, 1968.

25. Luxenberg, H. R. & Kuehn, R. L., Editors: Display Systems Engineering, McGraw-Hill, New York, 1968.

26. Mantell, C. L., Editor-in-Chief: Engineering Materials Handbook, 1st ed., McGraw-Hill, New York, 1958.

27. Mertz, L.: Transformations in Optics, John Wiley & Sons, New York, 1965.

28. Minnar, E. J., Editor: ISA Transducer Compendium, Plenum Publishing, New York, 1963.

29. National Academy of Sciences: "Fundamentals of Amorphous Semiconductors, Washington, D.C., 1972.

30. Norton, H. N.: Handbook of Transducers for Electronics Measuring Systems, Prentice-Hall, New Jersey, 1969.

31. Park, Y. S. and Reynolds, D. C.: "Exciton Structure in Photoconductivity of CdS, CdSe, and CdSiSe Single Crystals," Phys. Rev., Vol. 132, December 1963.

32. Pratt, W. K.: Laser Communications Systems, John Wiley & Sons, New York, 1969.

33. Ramon, C. V. and Nath, N. S. N.: "Analysis of Finite Dimensional Phase Gratings," Proc. Ind. Acad. Sci., Vol. 2A, 1935

34. Reimers, P.: "The Preparation of Graded-Band Single Crystals of II-VI Compounds," Phus. Stat. Sol., Vol. 35, 1969.

35. Royer, H.: "Holographic Velocimeter of Submicron Particles," Opt. Comm., Vol. 20, January 1977.

36. Shay, J. L. & Wernick, J. H.: Ternary Chalcopyrite Semiconductors: Growth, Electronic Properties, and Applications, Pergamon Press, Oxford, England, 1975.

37. Siemen, K. J. and Frenton, E. W.: "Optical Properties of Amorphous Selenium Films," Phys. Rev., 1967.

38. Skobel'tsyn, D. V., Editor: Luminescence and Nonlinear Optics, Proceedings (Trudy) of the P.N. Lebedev Physics Institude, Vol. 59, Plenum Publishing, New York, 1973.

39. Spear, W. E., et al: "Amorphous Silicon p-n Junction," Appl. Phys. Lett., Vol. 28, January 1976.

40. Thomas, D. G., et al: "Kinetics of Radiative Recombination at Randomly Distributed Donors and Acceptors," Phy. Rev., Vol. 140, October 1965.

41. Von Hipple, A. R., Editor: The Molecular Designing of Materials and Devices, The M.I.T. Press, Massachusetts Institute of Technology, Cambridge, Massachusetts, 1965.

42. Wheeler, R. G. and Goldberg, H. S.: "A Novel Voltage Tuneable Infrared Spectrometer-Detector," IEEE Trans., Vol. ED-22, November 1975

43. Willard, G. W.: "Bragg Condition Determination for Phase Gratings," Accoust. Soc. Am., Vol. 21, 1949.

44. Ziman, J. M.: Electrons and Phonons, Oxford University Press, London,. 1960.

APPENDIX A

HOLOGRAPHIC ANALYSES COMPUTER PROGRAM

```
TYPE OLD OR NEW:OLD:HOLO

OK
LIST


HOLO        11:01  RI T/S JAN 13, 1978

100  PRINT"3, 4 (ADD C-C0), OR 5 (ADD D2) OUTPUT COLUMNS?"
110  INPUT K
120  PRINT "VALUES OF P,Q"
130  INPUT P,Q
140  PRINT"T MIN,  T MAX,  T INCR"
150  INPUT T1,T2,T3
160  PRINT"MAXIMUM VALUE OF W"
170  INPUT W2
180  PRINT"Y MIN,Y MAX, Y INCR"
190  INPUT Y1,Y2,Y3
200  PRINT"VALUES OF N1,N FINAL,N INCR"
210  INPUT N1,N2,N3
220  LET L=P+Q
230  PRINT
231  PRINT
240  IF K=3 THEN 300
250  IF K=4 THEN 280
260  PRINT " N"," N-(C-C0)","   W","   C-C0","     D2"
261  PRINT " =","  ========","   =","   ====","     =="
270  GO TO 310
280  PRINT " N"," N-(C-C0)","   W","   C-C0"
281  PRINT "===","  ========","  ===","  ====="
290  GO TO 310
300  PRINT " N"," N-(C-C0)","   W"
301  PRINT "===","  ========","  ==="
310  FOR T=T1 TO T2 STEP T3
320  PRINT
321  PRINT
330  PRINT"****** THETA =",T,"********"
```

```
340  FOR Y=Y1 TO Y2 STEP Y3
350  PRINT
360  PRINT "VALUE OF Y:",Y
370  LET N=0
380  GOSUB 450
390  C0=C
400  PRINT"VALUE OF C0",C0
410  PRINT
420  FOR N=N1 TO N2 STEP N3
430  GOSUB 450
440  GO TO 620
450  LET W=10
460 LET D2=-L+SQR(W*W+P*P-2*P*W*SIN(T))+SQR(W*W+Q*Q+2*P*W*SIN(T))-N
490 IF D2*D2<1.0E-10 THEN 540
500 LET R1=(2*W-2*P*SIN(T))/(2*SQR(W*W+P*P-2*P*W*SIN(T)))
510 LET R2=(2*W+2*Q*SIN(T))/(2*SQR(W*W+Q*Q+2*Q*W*SIN(T)))
520 LET W=W-D2/(R1+R2)
530 GO TO 480
540 L5=P-W*SIN(T)
550 L6=W*COS(T)-Y
560 L1=SQR(L5*L5+L6*L6)
570 L7=Q+W*SIN(T)
580 L8=W*COS(T)+Y*Q/P
590 L2=SQR(L7*L7+L8*L8)
600 LET C=L1+L2-P-Q
610 RETURN
620 C5=N-(C-C0)
630 C5=INT(10000*C5)/10000
650 IF K=3 THEN 710
660 IF K=4 THEN 690
670 PRINT N,C5,W,C-C0,D2
680 GO TO 720
690 PRINT N,C5,W,C-C0
700 GO TO 720
710 PRINT N,C5,W
713 IF W<W2 THEN 720
714 N=N2+10
720 NEXT N
730 NEXT Y
740 NEXT T
750 END
```